DEVELOPMENT OF A REDUCED METHYL-CYCLOHEXANE MODEL FOR DIESEL ENGINE APPLICATIONS

TAN JOHNIN

A project report submitted in partial fulfilment of the requirements for the award of Bachelor of Engineering (Honours) Mechanical Engineering

Lee Kong Chian Faculty of Engineering and Science
Universiti Tunku Abdul Rahman

April 2019

DECLARATION

I hereby declare that this project report is based on my original work except for citations and quotations which have been duly acknowledged. I also declare that it has not been previously and concurrently submitted for any other degree or award at UTAR or other institutions.

Signature   :

Name   :   Tan Johnin

ID No.   :   14UEB05379

Date   :   29th April 2019

APPROVAL FOR SUBMISSION

I certify that this project report entitled **"DEVELOPMENT OF A REDUCED METHYL-CYCLOHEXANE MODEL FOR DIESEL ENGINE APPLICATIONS"** was prepared by **TAN JOHNIN** has met the required standard for submission in partial fulfilment of the requirements for the award of Bachelor of Engineering (Honours) Mechanical Engineering at Universiti Tunku Abdul Rahman.

Approved by,

Signature   :

Supervisor   :   Dr. Poon Hiew Mun

Date   :   29th April 2019

The copyright of this report belongs to the author under the terms of the copyright Act 1987 as qualified by Intellectual Property Policy of Universiti Tunku Abdul Rahman. Due acknowledgement shall always be made of the use of any material contained in, or derived from, this report.

ACKNOWLEDGEMENTS

First and foremost, I would like to express my gratitude to my research supervisor, Dr. Poon Hiew Mun for her invaluable advice, guidance and enormous patience throughout the development of the research.

In addition, I would also like to express my gratitude to my loving parents and friends who had helped and given me encouragement along the process of completing this project.

Last but not least, I would also like to express my gratefulness to UTAR for providing an opportunity to be involved in this research project.

ABSTRACT

Cyclo-alkanes are the major constituents of hydrocarbons in market fuels such as petrol, diesel, and aviation fuels. Diesel fuels derived from bituminous sands have up to 35 % of cyclo-alkanes. Furthermore, cyclo-alkanes play an important role in soot formation because they yield aromatic compounds through dehydrogenation. Hence, it is crucial to include cyclo-alkanes in diesel surrogate fuel models. As a result, better prediction in the combustion and emission simulations can be achieved. The aim of this study was to develop a reduced methyl-cyclohexane (MCH) model for diesel engine applications. In this study, the detailed MCH model with 1 540 species was served as the base model. The reduced MCH model was derived by performing mechanism reduction. Consequently, the reduced model with 86 species, namely MCHv1 was successfully derived after elimination of unimportant species. Next, MCHv1 was validated against detailed model with respect to ignition delay (ID) timings and species profiles in zero-dimensional (0-D) simulations. Computed results by MCHv1 were in close agreement with the detailed model. Maximum deviation in ID timings is only 28 %. Furthermore, the reduced model was validated against experimental results for jet-stirred reactor (JSR) and auto-ignition conditions. Simulated results using the reduced model were in close agreement with experimental data. Moreover, a reduced diesel surrogate fuel model with 144 species, namely D_144 was developed and MCHv1 was used to represent cyclo-alkanes. Lastly, D_144 surrogate model is ready to be used for parametrically study of combustion and pollutant formation in three-dimensional (3-D) internal combustion engine simulations and two-dimensional (2-D) spray combustion simulations.

TABLE OF CONTENTS

CHAPTER

LIST OF TABLES

LIST OF FIGURES

LIST OF SYMBOLS / ABBREVIATIONS

C_c	Consumption Rate Of Species c, mole/(m$^3 \cdot$ sec)
C_P	Specific Heat, J/(kg $\cdot$ K)
D_{MAX}	Maximum Tolerable Deviation
D_{ID}	Maximum Deviation in ID Timings
$\frac{dN_k}{dt}$	Build-Up Rate of Species k within the Reactor, mole/sec
E_a	Activation Energy, J/mol
E_t	Threshold Value
F_k^o	Inflow of Species k, mole/sec
F_k	Outflow of Species k, mole/sec
G_k	Production Rate of Species k within the Reactor, mole/sec
H	Enthalpy, J/mol
k_c	Equilibrium Constant
k_f	Forward Reaction Rate Constant
k_n	Leading Constant
k_r	Reverse Reaction Rate Constant
N_{rec}	Number of Reactions
N_{sp}	Number of Species
$N_{s,g}$	Total Number of Species in Path g
P_c	Production Rate of Species, mole/(m$^3 \cdot$ sec)
q	Rate of Progress for Reaction, mol/(m$^3 \cdot$ s)
R	Gas Constant, J/(mol $\cdot$ K)
r	Direct Interaction Coefficient
r_{cd}	Normalised Involvement of Species d to Production of Species c
R_{cd}	Overall Path-Dependent Coefficient
S	Entropy, J/mol
s_j	j^{th} Species: s_1 is Species c and s_{n_s} is Species d
$Sen_{normalised}$	Normalised Temperature Sensitivity Coefficient
Sen_i	Temperature A-Factor Sensitivity for i^{th} Reaction
Sen_{max}	Maximum Temperature A-Factor Sensitivity among All Reactions
T	Temperature, K
V	Volume of the Reactor, m^3

v	Overall Stoichiometric Coefficient of Species
$\dot{w}$	Production Rate of Species, mol/(m$^3 \cdot$ s)
X	Molar Concentration, mol/(m$^3 \cdot$ s)
v_k	Stoichiometric Coefficient of Species k
ω	Rate of Reaction, mole/(m$^3 \cdot$ sec)
$\delta_{d,k}$	Participation of Species d in k^{th} reaction
ϕ	Equivalence Ratio
0-D	Zero-Dimensional
2-D	Two-Dimensional
3-D	Three-Dimensional
ASTM	American Society for Testing Materials
C_2H_2	Acetylene
$C_6H_5CH_3$	Toluene
C_6H_6	Benzene
CHX	Cyclo-Hexane
CFD	Computational Fluid Dynamics
CO	Carbon Monoxide
CO_2	Carbon Dioxide
CN	Cetane Number
CSP	Computational Singular Perturbation
DIC	Direct Interdependency Coefficient
DOS	Diesel Oil Surrogate
DRG	Directed Relation Graph
DRGEP	DRG with Error Propagation
DRGASA	DRG-Aided Sensitivity Analysis
DRGEPSA	DRG with Error Propagation and Sensitivity Analysis
D_144	144 Species Reduced Diesel Surrogate Fuel Model
EN	European Standards
FYP	Final Year Project
GHG	Greenhouse Gases
H_2	Hydrogen

H$_2$O$_2$	Hydrogen Peroxide
HC	Hydrocarbon
HCO	Formyl
HMN	2,2,4,4,6,8,8-Heptamethylnonane
HO$_2$	Hydroperoxyl
HXN	N-Hexadecane
IARC	International Agency for Research on Cancer
ID	Ignition Delay
IDEA	Integrated Diesel European Action
ILDM	Intrinsic Low-Dimensional Manifolds
JSR	Jet-Stirred Reactor
MD	Methyl Decanoate
MCH	Methyl-Cyclohexane
MCHv1	86 Species Reduced Methyl-Cyclohexane Model
MCHv2	77 Species Reduced Methyl-Cyclohexane Model
N$_2$	Nitrogen
NO$_x$	Nitrogen Oxides
N_HEPT	N-Heptane
O$_2$	Oxygen
OH	Hydroxyl
PAH	Polycyclic Aromatic Hydrocarbons
PEA	Partial Equilibrium Assumptions
PCA	Principal Component Analysis
PM	Particulate Matter
PRF	Primary Reference Fuels
PSR	Perfectly-Stirred Reactor
QSS	Quasi-Steady-state
RCM	Rapid Compression Machine

LIST OF APPENDICES

APPENDIX	TITLE	PAGE

CHAPTER 1

INTRODUCTION

1.1   General Introduction

The history of diesel engines can be traced back to 1892 when the first design of compression ignition engine was patented by Rudolf Diesel. The main features of diesel engines are high compression ratio range from 12 to 24 (Gong, et al., 2016) and self-ignition of fuel takes place when subjected to high temperature compressed gas (Bae and Kim, 2016). Diesel engines are widely used in the industrial sector and transportation sector due to higher torque, better efficiency, lower carbon dioxide (CO_2) emissions and more durable compared to spark ignition engines (Hariram and Shangar, 2015; Jamrozik, et al., 2018).

However, the main problem of diesel engines is exhaust emissions such as CO_2, hydrocarbon (HC), particulate matter (PM), carbon monoxide (CO) and nitrogen oxides (NO_x). Diesel exhaust has harmful impacts on the environment and human health. For instance, CO_2 and NO_x are greenhouse gases (GHG) that accelerate global warming (Jamrozik, et al., 2018). In addition, PM is a poisonous particulate that highly inhalable owing to particle size smaller than 2.5 μm (Debia, et al., 2017; Iyogun, Lateef, and Ana, 2018). Besides, diesel exhaust is categorised as Class-1 carcinogens by the International Agency for Research on Cancer (IARC) according to the level of carcinogenicity (Rai, 2016). Carcinogens are chemical substances that capable to stimulate the formation of cancer. Hence, exposure to diesel exhaust can cause serious impact on health.

To meet the complex needs of society and strict emission regulations set by the government, it is necessary to continuously improve emissions and performance of diesel engines. Experimental measurements and numerical modelling are two common approaches used by the researchers to study the combustion processes and exhaust emissions particularly soot formation. The experimental approach is deemed to be time-consuming and costly because of the need to build prototype (Farrel, 2007). Numerical modelling especially computational fluid dynamics (CFD) simulation is convenient for studying the complex combustion and pollutant formation of the engines.

In the past decades, detailed chemical kinetic models are often incorporated into CFD simulation to explore the microscopic chemical processes and the macroscopic physical processes (Liao, et al., 2011). However, detailed models recently developed are not feasible to be used due to large number of species. For instance, the detailed 2-methyl alkanes model established by Sarathy, et al. (2011) comprises of 7 175 species. In addition, the computer processing time of simulation is proportional to the cube of number of species (Frassoldati, et al., 2015). Therefore, detailed mechanisms can cause problems, especially in multi-dimensional CFD simulation owing to large number of species. This had been demonstrated by Herbinet, et al. (2008), the detailed model of methyl decanoate (MD) comprises of 3 012 species was used in a motored engine simulation. The simulation took 160 hours to complete on computer with 4 GHz processor.

In short, detailed models are inappropriate to be used owing to high computational expenses and would eliminate the cost-effective advantage of CFD simulation. In light of this, mechanism reduction techniques were introduced to eliminate the unimportant species from detailed models while retaining adequate detail and accuracy. With advances in these techniques, the reduced models produced are able to achieve consistency between simulation and experimental results as well as minimise computational time.

1.2   Importance of the Study

With the increasing demand for high-efficiency diesel engines with low pollutant emissions, surrogate fuel models are widely used in CFD simulation to explore the combustion characteristics and exhaust emissions of diesel engines. Cyclo-alkanes are rarely included in diesel surrogate fuel models because their impacts on the ignitions are not significant. However, cyclo-alkanes play an important role in soot formation because they produce aromatic compounds by dehydrogenation. Besides, actual diesel fuels have up to 30 % of cyclo-alkanes. Hence, diesel surrogate fuel models without the representative of cyclo-alkanes are debatable.

It is desirable to include cyclo-alkanes in diesel surrogate fuel models. The reduced methyl-cyclohexane (MCH) model developed in this study can be employed to represent cyclo-alkanes in diesel surrogate fuel models. Therefore, better predictions in the combustion and emission behaviours can be achieved.

1.3   Problem Statement

Detailed chemical kinetic models usually contain thousands of species owing to comprehensiveness. The detailed MCH model that served as the base model of this study comprises of 1 540 species and 6 498 reactions. This detailed model is not suitable to be incorporated into multi-dimensional modelling especially in three-dimensional (3-D) simulation due to large mechanism size.

Besides that, chemical stiffness is another problem as the nonlinear coupling between species present in a detailed model. Hence, species and reactions that have insignificant impact on simulation results must be removed from the detailed model by applying mechanism reduction techniques. Consequently, computational efficiency can be improved by using the reduced model in numerical modelling.

1.4   Aim and Objectives

The aim of this study is to develop a reduced MCH model for diesel engine applications. The reduced MCH model must be capable to reproduce the simulation results consistent with the detailed MCH model. The key objectives of this study are:

   (i)   To determine the important species and main reaction pathways in the detailed MCH model.

   (ii)   To remove the unimportant species and reactions from the detailed model by applying the mechanism reduction techniques.

   (iii)   To compare the ignition delays (ID) timings and species profiles predictions between reduced model and detailed model.

1.5   Scope and Limitation of the Study

The scope of this study is to develop a reduced MCH model by using numerical analysis softwares: ANSYS CHEMKIN-PRO 19.0 and MATLAB R2018a. The limitations of this study are:

   (i)   Not involved in the development of detailed MCH model. The detailed MCH model by Weber, et al. (2014) is designated as the base model.

   (ii)   No experiment will be conducted in this study. Reduced model is validated against the experimental data in the literature.

1.6   Layout of the Report

In Chapter 1, a brief introduction to this project is described. Furthermore, the importance of study, problem statement, scopes and objectives are defined. The literature review of chemical kinetic mechanisms of diesel fuels and mechanism reduction techniques are presented in Chapter 2. Besides that, the detailed MCH model that serves as the base model of reduced model development is also reviewed.

Additionally, the methodology of reduced model development and work plan of the project are presented in Chapter 3. Furthermore, theoretical background and development processes of the reduced model are presented in Chapter 4. Finally, conclusions of the reduced model development and recommendations for future work are presented in Chapter 5.

CHAPTER 2

LITERATURE REVIEW

2.1   Introduction

Compositions of actual diesel fuel are described in Section 2.2. Then, the development of diesel surrogate fuel mechanisms is presented in Section 2.3. Chemical kinetic models of cyclo-alkane and the detailed model of MCH developed by Weber, et al. (2014), are presented in Section 2.4. Moreover, mechanism reduction approaches are described in Section 2.5. Additionally, key findings are concluded in Section 2.6.

2.2   Compositions of Actual Diesel Fuel

Diesel fuels typically are extracted from crude oil in the distillation operation at a temperature between 200 ℃ and 350 ℃. Diesel fuels comprise of roughly 25 % aromatic compounds and 75 % aliphatic compounds such as n-alkanes, naphthene and branched-alkanes (Huth and Heilos, 2013). The physicochemical properties of conventional diesel fuels are shown in Table 2.1.

Table 2.1: Properties of Conventional Diesel Fuels (Huth and Heilos, 2013)

Properties	Value
Carbon/Hydrogen Mass Ratio	86:14
Lower Heating Value (MJ/kg)	42.6
Flash Point (°C)	> 55
Density (kg/L)	$0.82 - 0.86$
Kinematic Viscosity at 40 °C (mm^2/s)	$2 - 5$

Other than crude oil, diesel fuels can be extracted from non-renewable resources such as coal, oil shale, natural gas, bituminous sands and petroleum coke. However, diesel fuels extracted from different sources have dissimilar in overall compositions. For instance, diesel fuels extracted from bituminous sands and coal contain more cyclo-alkanes as compared to crude oil derived diesel. Additionally,

diesel fuels extracted from natural gas and petroleum coke using the Fischer-Tropsch Synthesis mainly consist of iso-alkane and n-alkanes (Farrell, 2007).

Compositions of diesel fuels are different due to factors such as extraction sources and refinery standards (Qian, et al., 2018). For refinery standards, American Society for Testing Materials (ASTM) D975-16a of United States required minimum cetane number (CN) of 40, while European Standards (EN) 590:2009 of Europe mandatory the minimum CN of 51. Hence, it is essential to develop the diesel fuel surrogate models that able to manipulate threshold soot index and CN due to variation in fuel properties of market diesel fuels (Szymkowicza and Benajesb, 2018).

2.3 Development of Diesel Surrogate Fuel Mechanisms

Petroleum-derived products such as diesel, kerosene and gasoline are complex blends that contain diverse hydrocarbon species. Diesel fuels are $C_{10} - C_{24}$ hydrocarbons and the fuel constituents are comprised of $50 - 65\%$ n-alkanes and iso-alkanes, $20 - 30\%$ of cyclo-alkanes and $10 - 30\%$ of aromatics (Farrell, 2007). It is notable that the proportion of each fuel constituent is not fixed. Uncertainty of fuel compositions is an obstacle for diesel surrogate fuel mechanisms to precisely mimic the emissions formation of practical diesel fuels. For this reason, surrogate fuel mechanisms are usually developed for stimulating the combustion behaviours of engines (Qian, et al., 2018).

For the past decades, diesel surrogate fuel mechanisms can be categorised into two branches: chemical surrogate and physical surrogate. Physical surrogates are developed for replicating the physical features of practical diesel fuels while chemical surrogates are developed for replicating the chemical features which composed of main fuel constituents of practical diesel fuels (Edwards and Maurice, 2001). However, the engine combustion behaviour is controlled by both chemical and physical characteristic of practical diesel fuels. Therefore, a realistic surrogate fuel mechanism must capable to precisely emulate the fuel characteristics such as chemical constituents, H/C ratio, volatility, CN, density and molecular weight. Hence, the engine combustion behaviours such as performance, emissions, ignition and heat release can be predicted accurately (Colket, et al., 2007; Szymkowicza and Benajesb, 2018; Qian, et al., 2018).

Diesel surrogate fuel mechanisms are widely used in numerical modelling such as combustion simulation, spray characterization and chemical kinetic

modelling (Szymkowicza and Benajesb, 2018). Surrogate fuel mechanisms are the simplified representations of practical fuels. Single-component such as n-heptane (N_HEPT) and n-hexadecane are the simplest diesel surrogate fuel mechanisms (Pitz, et al., 2007). Single-component surrogate fuel mechanisms are the favourable choices in various diesel applications due to the restriction of computational expenses. Additionally, N_HEPT had been used extensively as representative of practical fuel due to its CN of 55 which is analogous with actual diesel fuels which range from 40 to 56 (Farrell, 2007; Poon, et al., 2016b; Chang, et al., 2015; Liu, et al., 2017). However, N_HEPT is more volatile than actual diesel fuel. Consequently, huge deviation in vaporization and liquid spray penetration, which eventually influence the local fuel/air ratio. Therefore, ignition behaviour of N_HEPT will not be in line with practical diesel fuel under an extensive range of speed/load (Farrell, 2007). After recognising the limitations of short-chain alkane such as N_HEPT, long-chain alkane such as n-hexadecane is developed due to their boiling range match with actual diesel fuels (Qian, et al., 2018; Poon, et al., 2016a).

Nonetheless, single-component surrogates of n-alkanes mechanisms cannot precisely replicate the combustion characteristics of the aromatic compounds, iso-alkanes and cyclo-alkanes that present in practical diesel fuels (Chang, et al., 2015). Besides, single-component surrogates do not describe well the formation of polycyclic aromatic hydrocarbons (PAH) (Poon, et al., 2016b). Therefore, single-component surrogates have smaller amount of soot productions than actual diesel fuels. To solve the shortcomings of single-component surrogates, binary, ternary and greater blend mechanisms with integrated of more fuel constituents such as Primary Reference Fuels (PRF), Integrated Diesel European Action (IDEA) and Diesel Oil Surrogate (DOS) have been developed (Chang, et al., 2015; Farrell, 2007; Poon, et al., 2016b; Szymkowicza and Benajesb, 2018).

2.4   Chemical Kinetic Mechanisms of Cyclo-Alkanes

Cyclo-alkanes are the major constituents of hydrocarbons that existing in market fuels such as petrol, diesel, and aviation fuels. With the rise in crude oil prices, bituminous sands become a favourable alternative due to its attractive economic value. However, transportation fuels derived from bituminous sands have higher proportion of cyclo-alkanes as compared to those of crude oil derived fuels (Sivaramakrishnan and Michael, 2009; Silke, et al., 2007; Pitz, et al., 2007). Diesel

fuels derived from bituminous sands have about 35 % of cyclo-alkanes. For that reason, ignition characteristics and pollutant emissions of diesel-powered engines are affected due to a significant increase in the cyclo-alkanes compound (Li et al, 2016; Silke, et al., 2007).

Furthermore, cyclo-alkanes play an important role in soot formation because they yield aromatic compounds through dehydrogenation as shown in Figure 2.1. As a consequence, aromatic compounds transform into the PAH which serves as a soot precursor (Sivaramakrishnan and Michael, 2009; Silke, et al., 2007). Therefore, understanding the oxidation paths and decomposition of cyclo-alkanes can subsequently improving the diesel surrogate fuel mechanisms in stimulating the engine combustion behaviours and soot formations. In the development of diesel surrogate fuel mechanisms, cyclo-hexane (CHX) frequently used to represent cyclo-alkanes owing to it is a simple structure of cyclo-alkanes (Poon, at al., 2016a).
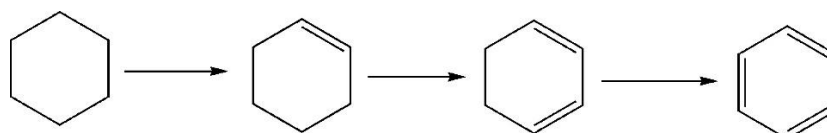
Figure 2.1: Formation of Benzene from Dehydrogenation of CHX (Silke, et al., 2007)

Chemical kinetic mechanisms and experimental measurements for cyclo-alkanes are limited in the past decade as reported in the literature. In recent year, there is a steady growth in the chemical kinetic mechanism for cyclo-alkanes. The CHX mechanism had been proposed by Dayma, et al. (2003), Sirjean, et al. (2007) and Bakali, et al. (2000) which applicable for high-temperature modelling. Besides that, CHX mechanism also proposed by Granata, et al. (2003), Buda, et al. (2006), Silke, et al. (2007), Cavallotti, et al. (2007), Zhang, et al. (2007) and Fernandes, et al. (2009) which applicable for both high and low temperature. It is noteworthy that, the CHX mechanism proposed by Zhang, et al. (2007) focused on the reactions path that directly yields benzene to emulate the PAH formation (Pitz, et al., 2011). Additionally, in the work of Fernandes, et al. (2009), molecular oxygen to the cyclohexyl radical path was considered as well as optimizing the rate constants had produced better prediction in ID timings. Apart from that, the alkyl cyclo-alkane such as MCH had gained attention in chemical kinetic mechanisms development.

MCH mechanism had been developed by Pitz, et al. (2007), Yang and Boehman (2009) and Weber, et al. (2014). The model developed by Pitz, et al. (2007) has successfully captured the ignition behaviour with slightly over-predicted in ignition time. Yang and Boehman (2009) proposed the detailed model of MCH, they also found out that reactivity of the fuel increased by the methyl group on the ring of MCH. Recently, the MCH mechanism developed by Pitz, et al. (2007) is updated with new reaction paths and rate constants by Weber, et al. (2014) and it showed substantial improvement in ID timing predictions. Review of the MCH mechanism developed by Weber, et al. (2014) will be discussed in Section 2.4.1 and it serves as the base model for the reduced MCH mechanism development.

2.4.1   Detailed Methyl-Cyclohexane Mechanism

The detailed MCH mechanism proposed by Weber, et al. (2014) is selected as the reference mechanism for the reduced MCH model development. This MCH mechanism comprises of 1 540 species and 6 498 reactions. It is an updated version of the detailed MCH mechanism developed by Pitz, et al. in 2007. It is noteworthy that the current mechanism has substantial improvement in ID timing predictions owing to revise of mechanism, especially in low-temperature chemistry.

Nonetheless, the model was validated against experimental measurements done by Mittal and Sung, (2009), Vasu, et al. (2009) and Vanderover and Oehlschlaeger (2009) in rapid compression machine (RCM) and shock tube conditions under an extensive range of conditions. The computed results and experimental results exhibited good agreement with uniform over-prediction in ID timings. However, the model was not validated against the experimental data for flame conditions.

This detailed MCH mechanism was developed founded on the $C_1 - C_6$ mechanism constructed by Curran, et al. (2002). Additional species and reactions for high and low temperature chemistry of MCH were incorporated into the mechanism. Besides, several sub-mechanisms of the $C_1 - C_6$ mechanism have been replaced with the recently established mechanisms. Firstly, the $C_1 - C_4$ mechanism was replaced with AramcoMech version 1.3 which developed by Metcalfe, et al. (2013). Moreover, CHX sub-mechanism was replaced with the mechanism proposed by Silk, et al. (2007). Next, aromatics base chemistry is based on LLNL-NUIG model proposed by Nakamura, et al. (2014).

Nevertheless, high-temperature reactions of MCH developed by Orme, et al. (2005) were added into the mechanism. These high-temperature reactions had been well validated against ID timings in shock tube and species concentration in a flow reactor. Besides, MCH abstractions rates were adjusted by referring to the experimental measurement done by Sivaramakrishnan and Michael (2009) as well as LLNL reaction rate rules (Sarathy, et al., 2011).

2.5   Chemical Kinetic Mechanism Reduction Techniques

Detailed chemical kinetic mechanisms are not suitable to be incorporated into multidimensional modelling due to high computational expenses as a large number of species and reactions. For instance, the detailed 2-methyl alkanes mechanism established by Sarathy, et al. (2011) comprises of 31 669 reactions and 7 175 species (Stagni, et al., 2016). Furthermore, chemical stiffness is induced by nonlinear coupling and wide ranges of time scales between species are present in a detailed model (Chen and Chen, 2016). Species present in a detailed model can be characterised into three categories: important, marginal and unimportant when operating conditions such as equivalence ratio, temperature and pressure are specified (Stagni, et al., 2016; Xin, et al., 2014). Hence, unimportant species and reactions can be removed by using mechanism reduction techniques while retaining adequate detail and accuracy (Ra and Reit, 2008). Mechanism reduction techniques can be grouped into three main categories: skeletal mechanism reduction, time-scale analysis and isomer lumping (Lu and Low, 2009).

2.5.1   Skeletal Mechanism Reduction Techniques

The first method is skeletal mechanism reduction; it used to remove unimportant species and reactions that have an insignificant impact on simulation results from the detailed model. It is favourable to be employed in the initial reduction (Niemeyer, et al., 2010). Mechanism reduction techniques for the classical skeletal mechanism reduction are Sensitivity Analysis (Rabitz, et al., 1983), Principal Component Analysis (PCA) (Vajda, et al., 1985), and Detailed Reduction (Wang and Frenklach, 1991).

The recent skeletal mechanism reduction techniques are Optimization (Bhattacharjee, 2003), Directed Relation Graph (DRG) (Lu and Law, 2005), DRG with Error Propagation (DRGEP) (Pepiot and Pitsch, 2008), DRG-aided Sensitivity

Analysis (DRGASA) (Sankaran, et al., 2007; Zheng, et al., 2007) and DRG with Error Propagation and Sensitivity Analysis (DRGEPSA) (Niemeyer, et al., 2010).

Sensitivity Analysis developed by Rabitz, et al. (1983) is one of the traditional skeletal mechanism reduction techniques. It is a simple method but needs exhaustive post-processing to run decoupled information regarding the reactions and species. Next, PCA proposed by Vajda, et al. (1985) is a technique used to remove unwanted reactions and users are required to reasonably designated reduction criterion to regulate the accuracy. The Detailed Reduction proposed by Wang and Frenklach (1991) identifies unimportant reactions by comparisons of reaction rates with self-defined critical values but this method tends to disregard important radicals with slow reaction rate.

Optimization developed by Bhattacharjee (2003) was proposed to recognise an optimum number of reactions under given constraints but asymptotically slower as compared to Sensitivity Analysis (Ra and Reit, 2008). Recently, DRG and DRG-based methods were introduced and ought to be effective methods among skeletal mechanism reduction techniques. This is because the classical skeletal mechanism reduction techniques are deemed to be computationally expensive while DRG and DRG-based techniques are straightforward, effective reduction techniques as well as able to deal with bigger size mechanisms (An and Jiang, 2013). Besides, DRG and DRG-based techniques are effective for the initial reduction of large size models owing to their efficient characteristics (Chen and Chen, 2016).

DRG was introduced by Lu and Low in 2005, the graph-searching approach is used to determine the species with strong coupling with major species and identify the unessential species for removal based on the predetermined tolerable error threshold and target species (Lu and Low, 2009; Niemeyer, et al., 2010). Next, DRG estimates the significance of the other species in contribution to the formation of target species (Stagni, et al., 2016). DRG does not produce the smallest mechanism but it is a famous method for reduction of large detailed model owing to low computational demand (Niemeyer et al 2010; Tosatto et al., 2013).

There are numerous methods have been introduced based on DRG methodologies such as DRGEP, DRGASA and DRGEPASA. DRGEP proposed by Pepiot and Pitsch in 2008 aims to overcome the shortcoming of DRG by considering the propagation of error induced by removal of species that deemed to be undesired.

However, DRGEP unable to identify all unessential species when fast production and consumption happen concurrently (Gao, et al., 2016). Nonetheless, DRGASA proposed by Sankaran, et al. (2007) and Zheng, et al. (2007) by fused sensitivity analysis into the DRG method.

DRGASA is capable to further reduce the mechanisms and resulting reduced models are much smaller as compared to DRG. However, DRGASA tends to safeguard unimportant species from removal. Nevertheless, DRGEPSA had been proposed by Niemeyer, et al. in 2010 and it is a fusion between DRGEP and DRGASA. This had been demonstrated in the reduction of N_HEPT model, DRGEPSA harvests a smaller size model as compared to DRGASA when given an identical simulation error (Li, et al., 2016).

Last but not least, sensitivity-based reduction techniques such as DRGASA and DRGEPSA need higher calculating demand because the sensitivity of each species is assessed based on a one-by-one examination (Stagni, et al., 2016; Li, et al., 2016). The strengths and weaknesses of the skeletal mechanism reduction methods are tabulated in Table 2.2.

Table 2.2: Strengths and Weaknesses of the Skeletal Mechanism Reduction Methods

Types of Skeletal Mechanism Reduction Methods	
1. Sensitivity Analysis by Rabitz, et al., 1983	
Strength: Simple method	*Weakness:* Extensive post-processing to run decoupled information
2. PCA by Vajda, et al., 1985	
Strength: Able to regulate the accuracy	*Weakness:* Users are required to reasonably designated reduction criterion
3. Detailed Reduction by Wang and Frenklach, 1991	
Strength: Eliminates reactions by comparisons of reaction rates	*Weakness:* Disregard important radicals with the slow reaction rate

Table 2.2 (Continued)

4. Optimization by Bhattacharjee, 2003	
Strength:	*Weakness:*
Recognises an optimum number of reactions under given constraints	Requires high computational expenses

5. DRG by Lu and Law, 2005	
Strength:	*Weakness:*
Effective reduction techniques to deal with large size mechanisms	Estimates the significance of the other species in involvement in the formation of target species

6. DRGEP by Pepiot and Pitsch, 2008	
Strength:	*Weakness:*
Overcomes the shortcoming of DRG by considering the propagation of error	Unable to identify all unessential species when fast production and consumption happen concurrently

7. DRGASA by Sankaran, et al., 2007; Zheng, et al., 2007	
Strength:	*Weakness:*
Reduced models are much smaller as compared to DRG	Tends to safeguard unimportant species from removal

8. DRGEPSA by Niemeyer, et al., 2010	
Strength:	*Weakness:*
Harvests a smaller mechanism than DRGASA	High computational demand

2.5.2 Time Scale Reduction Techniques

The second method is the time-scale analysis; it used to reduce the number of transported variables by time-scale reduction (Lu and Low, 2009). It recognises the fast species and reactions and represents their time developments by algebraic equations (Xin, et al., 2014). Consequently, the chemical stiffness of the mechanism can be reduced (Perini, et al., 2012). Mechanism reduction techniques for time-scale analysis are Quasi-Steady-State (QSS) (Montgomery, et al, 2006), Partial Equilibrium Assumptions (PEA) (Chen, 1988; Sung, et al., 2001), Intrinsic Low-Dimensional Manifolds (ILDM) (Maas and Pope, 1992) and Computational Singular

Perturbation (CSP) (Valorani, et al., 2006; Lam and Coussis, 1989). QSS analysis presumes that quick exhausting species can rapidly achieve and persist in low concentration. Hence, the QSS species derived have lower reaction rate than those of non-QSS species. PEA presumes that the rapid reactions are stable by counter reactions if they are unrestricted by exhausted reactant. ILDM and CSP are built on Jacobian analysis; they can decouple both slow and fast subspaces, but require high computational expenses (Lu and Low, 2009).

Besides, time-scale analysis methods are derived from complicated mathematical and often pose problems for an average user to apply (An and Jiang, 2013). The strengths and weaknesses of the time scale reduction methods are tabulated in Table 2.3.

Table 2.3: Strengths and Weaknesses of the Time Scale Reduction Methods

Types of Time Scale Reduction Methods	
1. PEA by Chen, 1988; Sung, et al., 2001	
Strength: An efficient method for chemical stiffness removal	*Weakness:* Partial equilibrium reactions require to be determined accurately
2. ILDM by Maas and Pope, 1992	
Strength: Handle the fast species brought by partial equilibrium reactions	*Weakness:* High computational demand for reduction of large mechanisms
3. CSP by Lam and Coussis, 1989; Valorani, et al., 2006	
Strength: Offers a fine-tuning way to decouple the fast and slow subspace	*Weakness:* High computational expenses owing to CSP refinement
4. QSS by Montgomery, et al, 2006	
Strength: Recognises an optimum number of reactions under given constraints	*Weakness:* Requires high computational expenses

2.5.3 Isomer Lumping

The third method is isomer lumping, it reduces the complexity of mechanism by substituting reactions of isomers with a reduced set of lumped virtual species. Lumping is a prevailing method for minimising the size of mechanisms while preserves the important elements of original mechanisms (Ra and Reitz, 2008). For instance, N_HEPT yields produce four heptyl radicals via dehydrogenation. The reaction of these radicals can be lumped into a representative reaction (Hernández, et al., 2014).

Lumping technique is favourable for mechanism with large carbon number owing to the presence of large amount of isomeric species. Isomers generally have comparable transport and thermal properties. Hence, their transport equations can be clustered. Besides, the presence of isomers in mechanism may lead to replicated reactions, lumping decreases the number of reactions when parallel reaction paths are present. As a result, the computational expenses can be lowered especially for calculations that involved diffusion, inter-process communication and Jacobian matrix. However, usage of the isomer lumping method is prohibited when locally originated projectors are time-dependent as well as firmly system (Lu and Low, 2009).

2.5.4 Integrated Reduction Techniques

Detailed models generally have more than thousands of species and reactions owing to comprehensiveness. However, time scales of the species in the detailed model have huge variations. Big difference in time scales encouraged chemical stiffness in simulations. Hence, bulky size detailed models are not feasible to incorporate into simulations.

In light of this, reduction techniques can be employed to get rid of redundant species and reactions. However, detailed models reduced by single-technique are still no viable to be used in multi-dimensional combustion simulations. Therefore, the multiple-technique namely integrated technique can be utilised to reduce detailed models until an extent that mechanisms are ready to be used in the application of multi-dimensional combustion simulations (Lu and Low, 2009). Recently, integrated techniques have to gain plentiful attention in chemical kinetic mechanism reduction and have been introduced by Lu and Low (2008), Hernández, et al. (2014) and Poon, et al. (2013).

In the work of Lu and Low in 2008, an integrated technique was proposed as shown in Figure 2.2. Two skeleton mechanism reduction techniques which are DRG and DRGASA were employed to reduce a detailed model of N_HEPT with 2 539 reactions and 591 species. By applying DRG as well as DRGASA, 483 species and 2 180 reactions were removed. Next, the mechanism was further reduced to 55 species and 51 global-steps by eliminating unnecessary reaction, isomer lumping as well as QSS analysis.
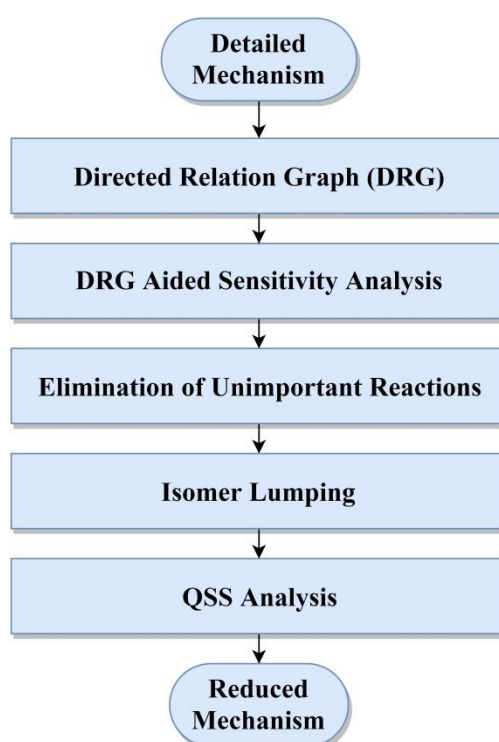
Figure 2.2: Integrated Technique Proposed by Lu and Low (2008)

Next, Hernández, et al. (2014) developed a novel integrated technique where three-technique: DRGEP, reactions analysis and isomer lumping techniques were combining in series as shown in Figure 2.3. Besides, the proposed integrated technique was used in the reduction of the detailed diesel surrogate model with 3 316 reactions and 772 species. Firstly, DRGEP was used to reduce the detailed surrogate model to 544 species and 2 503 reactions. Then, the model was further reduced to 436 species and 1 369 reactions through reaction analysis reduction. Finally, a reduced diesel surrogate model with 288 species and 1 072 reactions was attained after isomer lumping.
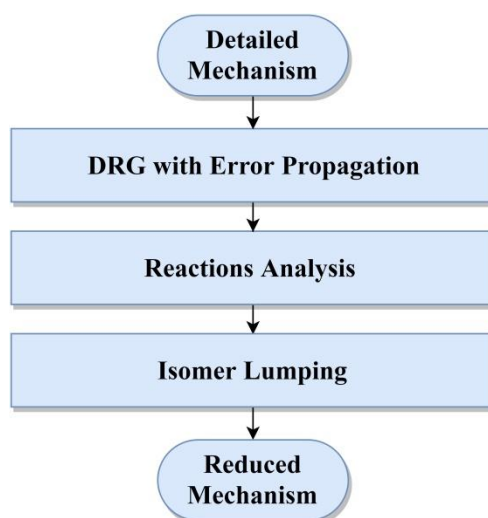
Figure 2.3: Integrated Technique Proposed by Hernández, et al. (2014)

Nevertheless, a five-stage mechanism reduction scheme was introduced by Poon, et al. (2013) which comprises of five techniques: DRGEP, isomer lumping, analysis of reaction path, DRG and rate constant adjustment as shown in Figure 2.4. In the work of Poon, et al. (2013), the integrated technique was applied in reduction of biodiesel surrogate as well as the reduction of diesel surrogate. The resulting reduced models were able to reproduce the ignition behaviour and in good agreement of results with detailed models.
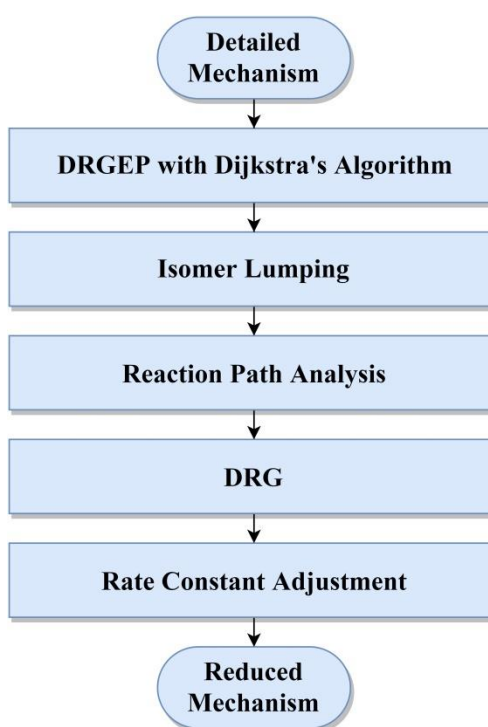
Figure 2.4: Integrated Technique Proposed by Poon, et al. (2013)

2.6   Summary

From the literature review, it is noticed that multi-component diesel surrogate fuel models will be relevant in the future because they can predict the combustion characteristics of market fuel more accurate than the single-component diesel surrogate fuel models. Besides, it is noted that cyclo-alkanes presence with a considerable amount in market fuel. Cyclo-alkanes play a key role in soot formation. Hence, it is crucial to include cyclo-alkanes in diesel surrogate models.

Furthermore, there is a trend of increasing in size of detailed chemical kinetic mechanisms and these mechanisms are not suitable to be incorporated into multi-dimensional modelling owing to large amount of species and reactions. For example, the detailed MCH model that used in this study comprises of 1 540 species and 6 498 reactions. Consequently, mechanisms reduction techniques are introduced to downsize the detailed models until an extent it is feasible to be employed in multi-dimensional simulations. Last but not least, integrated techniques are found to be more appropriate for large scale reduction of the detailed models.

CHAPTER 3

METHODOLOGY AND WORK PLAN

3.1   Introduction

Work plan for this final year project (FYP) and methodology of reduced model development are outlined in this chapter. In Section 3.2, important tasks in this project are identified, and the scheduling of the project is made using the Gantt chart. In Section 3.3, an overall flow of the reduced MCH model development is proposed.

3.2   Project Planning

The overall workflow of the project is shown in Figure 3.1. Next, tasks in FYP part 1 and part 2 are scheduled as shown in Figure 3.2 and Figure 3.3, respectively.
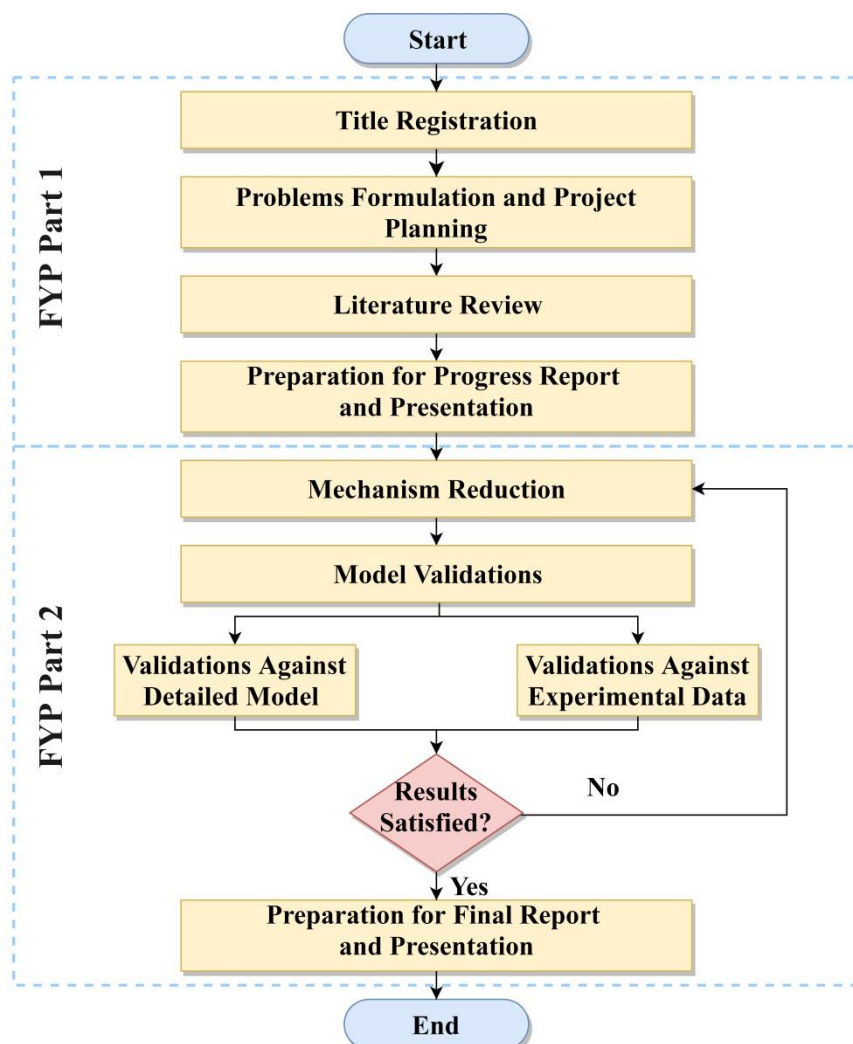
Figure 3.1: Flow Chart of the Project Work Plan

The Gantt chart of the project work plan for May trimester in 2018 is shown in Figure 3.2. The first task is title registration which falls on week 1 of the trimester. After registering for the FYP title, problems are formulated and planning for the project is carried out. Next, a comprehensive literature review is performed as well as the methodology is formulated. Lastly, progress report and presentation are prepared.

	Task Name	Duration	Start Time	Due Date	May Trimester 2018 (Week) 1 2 3 4 5 6 7 8 9 10 11 12 13 14
1	FYP Part 1	14 weeks	28/05/2018	02/09/2018	
1.1	Title Registration	1 week	28/05/2018	03/06/2018	
1.2	Problem Formulation	1 week	04/06/2018	10/06/2018	
1.3	Project Planning	1 week	11/06/2018	17/06/2018	
1.4	Literature Review	5 weeks	18/06/2018	22/07/2018	
1.5	Methodology Formulation	2 weeks	23/07/2018	05/08/2018	
1.6	Preparation for Report	2 weeks	06/08/2018	19/08/2018	
1.7	Preparation for Presentation	2 weeks	20/08/2018	02/09/2018	

Figure 3.2: Gantt Chart of the Project Work Plan for May Trimester in 2018

Figure 3.3 shows the Gantt chart of the project work plan for January trimester in 2019. Mechanism reduction is conducted from week 1 to week 8 by performing DRGEP, isomer lumping, reaction path analysis, DRG and A-factor adjustments. Once the reduced model is successfully developed, simulations will be performed and results are analysed. Finally, the results are documented in the final report and presentation is prepared.

	Task Name	Duration	Start Time	Due Date	Jan Trimester 2019 (Week) 1 2 3 4 5 6 7 8 9 10 11 12 13 14
2	FYP Part 2	14 weeks	14/01/2019	19/04/2019	
2.1	DRGEP Reduction	2 weeks	14/01/2019	27/01/2019	
2.2	Isomer Lumping	1 week	28/01/2019	03/02/2019	
2.3	Reaction Path Analysis	2 weeks	04/02/2019	17/02/2019	
2.4	DRG Reduction	1 week	18/02/2019	24/02/2019	
2.5	A-factor Adjustments	2 weeks	25/02/2019	10/03/2019	
2.6	Model Validations	2 weeks	11/03/2019	24/03/2019	
2.7	Preparation for Report	3 weeks	25/03/2019	14/04/2019	
2.8	Preparation for Presentation	1 week	15/04/2019	19/04/2019	

Figure 3.3: Gantt Chart of the Project Work Plan for Jan Trimester in 2019

3.3 Reduced Methyl-Cyclohexane Model Development Plan

An outline of the reduced MCH model development plan is shown in Figure 3.4. Firstly, a base model and an integrated reduction technique are selected after the comprehensive literature review. Then, mechanism reduction is performed by applying an integrated reduction technique on the detailed MCH model. Nevertheless, the reduced model is then validated against detailed model and experimental data. The details of each step are discussed in the following subsections.
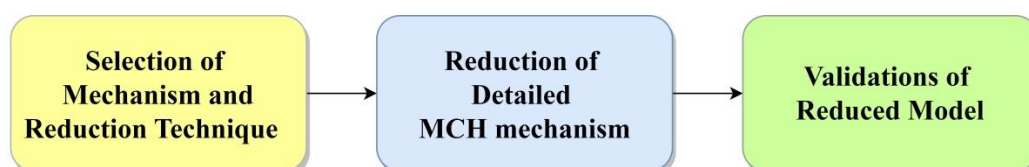
Figure 3.4: Flow Chart of the Reduced MCH Model Development Plan

3.3.1 Selection of Model and Reduction Technique

Figure 3.5 shows the steps involved in the selection of model and reduction technique. Firstly, the study and research on existing MCH models and techniques are presented in the literature review of Chapter 2. After comparing the existing reduction techniques and detailed models, five-stage reduction scheme proposed by Poon, et al. (2013) and detailed MCH model developed by Weber, et al. (2014) were selected.
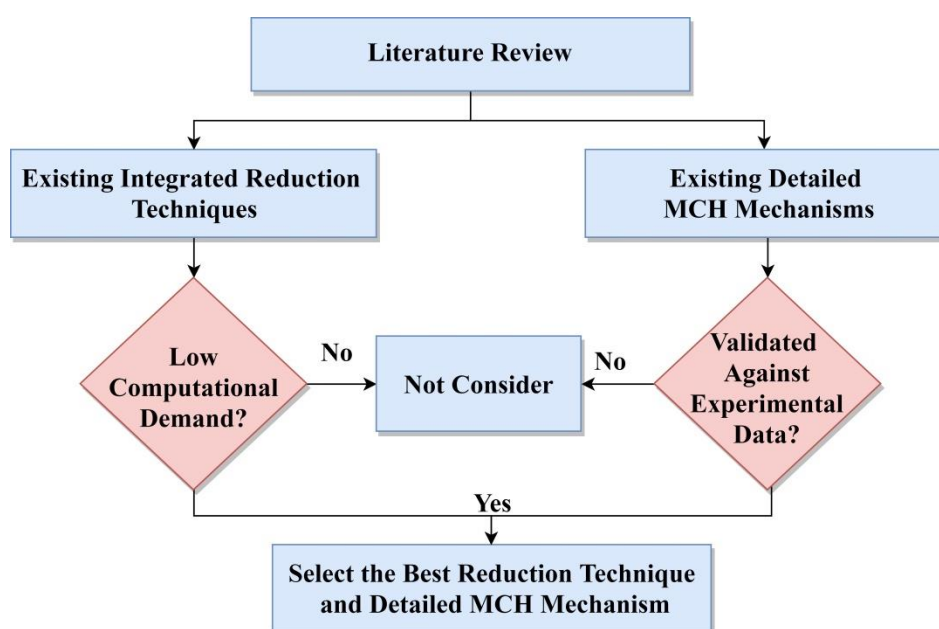
Figure 3.5: Flow Chart of the Selection of Mechanism and Reduction Technique

3.3.2   Reduction of the Detailed Methyl-Cyclohexane Model

In mechanism reduction, the detailed MCH model is reduced by applying the five-stage reduction scheme as shown in Figure 3.6. Firstly, the DRGEP using Dijkstra's algorithm is employed in the first step of mechanism reduction. The chosen target species are CO, CO_2, HCO, HO_2, H_2O_2, H_2, N_2, C_2H_2, C_6H_6 and $C_6H_5CH_3$. CO and CO_2 are the key emission species. HO_2 radical, HCO, H_2O_2 species are vital in chain branching reactions. H_2 are chosen to permit a larger degree of reduction and N_2 is representative of inert species. Besides, C_2H_2 is the precursor species of soot formation. Lastly, C_6H_6 and $C_6H_5CH_3$ are chosen to preserve the aromatic chemistries of the detailed model.

Figure 3.6: Flow Chart of the Mechanism Reduction

Next, isomer lumping is performed after the DRGEP mechanism reduction. It used to lump isomers with same transport and thermodynamic properties into a single pseudo species. Moreover, isomers with low production rate are removed. Subsequently, the reaction pathways in the mechanism are evaluated to further reduce the mechanism. Reactions with small normalised sensitivity are eliminated owing to they have insignificant influence on the production of connecting species.

Furthermore, the DRG is adopted to remove unwanted species that off tracked the reaction paths as the result of isomer lumping and reaction path analysis. Finally, reaction rate constants are tuned to optimise the reduced model and improve the ID timing predictions.

3.3.3 Validations of Reduced Model

In this section, the reliability of the reduced model is examined by performing zero-dimensional (0-D) simulations. The flow chart of reduced model validations is shown in Figure 3.7.
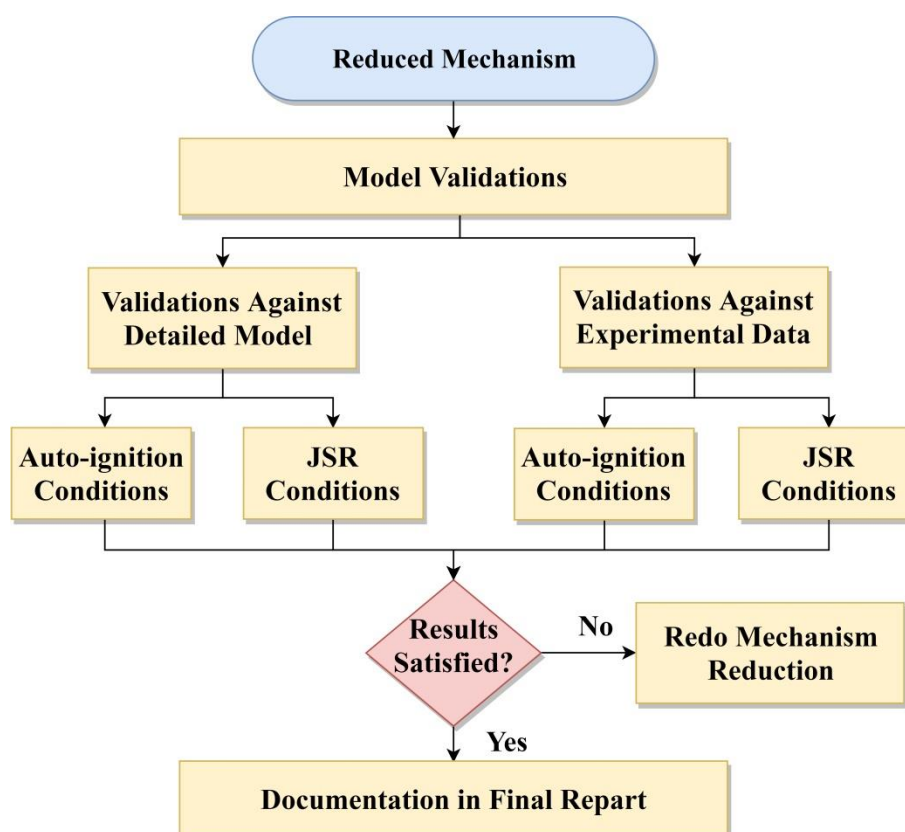
Figure 3.7: Flow Chart of Model Validations

First and foremost, the reduced model is validated against detailed model in ID timing predictions as well as species moles fraction predictions. It is done by performing 0-D simulations in CHEMKIN-PRO software. Simulations are performed under conditions of the jet-stirred reactor (JSR) and auto-ignition by using perfectly-stirred reactor (PSR) model and closed homogeneous batch reactor model, respectively. Nonetheless, the reduced model is validated against experimental data.

3.4   Concluding Remarks

According to the work plan presented in this chapter, the literature review is scheduled to be finished by the end of FYP Part 1. Subsequently, the development of a reduced model is initiated at the commencement of FYP Part 2. In the development of the reduced model, five-stage mechanism reduction scheme proposed by Poon, et al. (2013) was selected to reduce the detailed MCH mechanism developed by Weber, et al. (2014).

CHAPTER 4

FORMULATION OF A REDUCED METHYL-CYCLOHEXANE MODEL

4.1   Introduction

Theoretical background and development processes of the reduced model are presented in this chapter. In Section 4.2, background theories of chemical kinetics, reactor models as well as mechanism reduction techniques are described. Then, test conditions used in mechanism reduction and model validations are presented in Section 4.3. Subsequently, derivations and further validations of the reduced model are presented in Section 4.4 and Section 4.5, respectively. In addition, the formulation of a reduced diesel surrogate fuel model is presented in Section 4.6. Finally, the results obtained are discussed in Section 4.7.

4.2   Theoretical Background

This section introduced the theories related to this study. These theories such as chemical kinetics and mass balance of reactors are applied in the CHEMKIN-PRO simulations. First, the theoretical backgrounds of chemical kinetics are discussed in Section 4.2.1. Then, mass balance equations of the open PSR and closed homogeneous batch reactor are presented in Section 4.2.2 as these two reactors are employed in the kinetic studies. In Section 4.2.3, the theoretical backgrounds of skeletal mechanism reduction techniques are discussed.

4.2.1   Chemical Kinetics

Development of mechanism involves an understanding of the reaction paths for fuel and oxidation and pyrolysis. Chemical kinetics mechanisms developed are content with important descriptions for thermodynamic properties and chemical reactions.

Thermodynamic properties of all gaseous species are stored in DAT file format. Information that stored inside can be utilised to calculate enthalpy, entropy and specific heat as shown in equations below.

$$C_P = R\left(k_1 + k_2 T + k_3 T^2 + k_4 T^3 + k_5 T^4\right)$$

(4.1)

$$H = RT\left(k_1 + \frac{k_2 T}{2} + \frac{k_3 T^2}{3} + \frac{k_4 T^3}{4} + \frac{k_5 T^4}{5} + \frac{k_6}{T}\right) \tag{4.2}$$

$$S = R\left(k_1 \ln T + k_2 T + \frac{k_3 T^2}{2} + \frac{k_4 T^3}{3} + \frac{k_5 T^4}{4} + k_7\right) \tag{4.3}$$

where

C_P = specific heat, J/(kg · K)

R = gas constant, J/(mol · K)

T = temperature, K

k_n = leading coefficient

H = enthalpy, J/mol

S = entropy, J/mol

Furthermore, the production rate of species i^{th} in x^{th} reaction is expressed in Equation 4.4 and Equation 4.5. Besides, it is influenced by the forward and reverse reaction rate.

$$\dot{w}_i = \sum_{x=1}^{N_{rec}} v_{ix} q_x \tag{4.4}$$

$$\dot{w}_i = \sum_{x=1}^{N_{rec}} v_{ix} \left(k_{f,x} \prod_i^{N_{sp}} (X_i)^{v'_{ix}} - k_{r,x} \prod_i^{N_{sp}} (X_i)^{v''_{ix}}\right) \tag{4.5}$$

where

$\dot{w}$ = production rate of species, mol/(m^3 · s)

N_{rec} = number of reactions

N_{sp} = number of species

v = overall stoichiometric coefficient of species

q = rate of progress for reaction, mol/(m^3 · s)

X = molar concentration, mol/(m^3 · s)

k_f = forward reaction rate constant

k_r = reverse reaction rate constant

In addition, the forward reaction rate constant can be calculated by using 3 Arrhenius parameters as shown in Equation 4.6. Then, the reverse reaction rate constant is the division of the forward reaction rate constant and the equilibrium constant as expressed in Equation 4.7.

$$k_f = AT^\beta \exp(-\frac{E_a}{RT}) \qquad (4.6)$$

$$k_r = \frac{k_f}{k_c} \qquad (4.7)$$

where

k_f = forward reaction rate constant

k_r = reverse reaction rate constant

k_c = equilibrium constant

A = pre-exponential factor, (mole $\cdot$ cm $\cdot$ sec $\cdot$ K)

β = temperature exponent

E_a = activation energy, cal/mol

R = gas constant, J/(mol $\cdot$ K)

T = temperature, K

4.2.2 Reactor Models

In CHEMKIN-PRO software, PSR reactor model and closed homogeneous batch reactor model are used in 0-D simulations to simulate auto-ignition and JSR conditions, respectively. Next, network diagrams of both reactor models are shown in Figure 4.1. By performing control volume analysis as shown in Figure 4.2, with the assumption made that the system is adiabatic whereby no heat losses from the system and no heat transfers from surrounding.
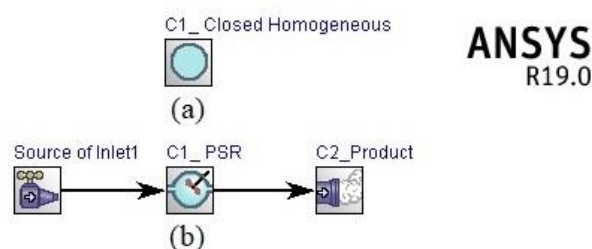
Figure 4.1: Network Diagrams of (a) Closed Homogeneous Batch Reactor and (b) PSR Reactor
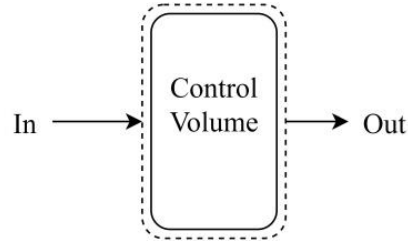
Figure 4.2: Control Volume Analysis of the Reactor

General equations of mole balance on the reactor for species k are expressed as below, where the accumulation of species k is equal to inlet mole flow rate plus the rate of production inside the reactor and deducts with outlet mole flow rate.

$$\underbrace{\frac{dN_k}{dt}}_{\text{Accumulation}} = \underbrace{F_k^o}_{\text{In}} - \underbrace{F_k}_{\text{Out}} + \underbrace{G_k}_{\text{Genaration}} \tag{4.8}$$

$$G_k = v_k \omega V \tag{4.9}$$

$$\frac{dN_k}{dt} = F_k^o - F_k + v_k \omega V \tag{4.10}$$

where

F_k^o = inflow of species k, mole/sec

F_k = outflow of species k, mole/sec

G_k = production rate of species k within the reactor, mole/sec

$\frac{dN_k}{dt}$ = build-up rate of species k within the reactor, mole/sec

v_k = stoichiometric coefficient of species k

ω = rate of reaction, mole/(m^3·sec)

V = volume of the reactor, m^3

First and foremost, closed homogeneous batch reactor model is used in this study to simulate the transient state of the system as governing variables are changing with time. Hence, the mole fraction of key species and ID timings are calculated as a function of time. Batch reactors have neither outflow nor inflow of products: $F_k^o = F_k = 0$. If reaction substances of reactors are perfectly mixed, Equation 4.10 can be rewritten as:

$$\frac{dN_k}{dt} = v_k \omega V \tag{4.11}$$

where

G_k = production rate of species k within the reactor, mole/sec

$\frac{dN_k}{dt}$ = build-up rate of species k within the reactor, mole/sec

v_k = stoichiometric coefficient of species k

ω = rate of reaction, mole/(m^3·sec)

V = volume of the reactor, m^3

Furthermore, PSR model is utilised in this study to simulate the steady-state of the system. Therefore, the mole fraction of key species is obtained as a function of temperature. PSR is working at steady-state whereby conditions do not vary with time: $\frac{dN_k}{dt} = 0$. If reaction substances of reactors are flawlessly mixed, Equation 4.10 can be rewritten as:

$$F_k^o - F_k = v_k \omega V \tag{4.12}$$

where

F_k^o = inflow of species k, mole/sec

F_k = outflow of species k, mole/sec

v_k = stoichiometric coefficient of species k

ω = rate of reaction, mole/(m^3·sec)

V = volume of the reactor, m^3

4.2.3 Mechanism Reduction Techniques

Two skeletal mechanism reduction techniques are applied in the reduction procedure: DRG and DRGEP.

DRG was introduced by Lu and Low in 2005, a graph-searching approach is used to determine the species with strong coupling with major species. In DRG, a normalised involvement, r_{cd} is used to measure the significance of species d to production of species c, and it is expressed as:

$$r_{cd} = \frac{\sum_{k=1,N_{rec}} |v_{c,k}\omega_k\delta_{d,k}|}{\sum_{k=1,N_{rec}} |v_{c,k}\omega_k|} \tag{4.13}$$

where

r_{cd} = normalised involvement of species d to production of species c

N_{rec} = total number of reactions

$v_{c,k}$ = stoichiometric coefficient of species k

ω_k = rate of reaction of kth reaction, mole/(m^3·sec)

$\delta_{d,k}$ = participation of species d in k^{th} reaction

The participation of species d in k^{th} reaction, $\delta_{d,k}$ is equal to 1 if species d participates in k^{th} reaction, and assigned to 0 if in k^{th} reaction does not involves species d. Removal of unessential species is based on the predetermined tolerable error threshold, E_t. Species with $r_{cd} < E_t$ are then removed from the mechanism. In the reduction procedure, DRG is adopted and E_t is set to unity to remove unwanted species that off tracked the reaction paths as the result of isomer lumping and reaction path analysis.

Next, DRGEP was proposed by Pepiot and Pitsch in 2008, and a Direct Interdependency Coefficient (DIC) is introduced to quantify the coupling between two species in reference to the consumption and production rate. DIC is expressed as:

$$\text{DIC} = \frac{\sum_{k=1,N_{rec}} |v_{c,k}\omega_k\delta_{d,k}|}{\max{(P_c,C_c)}} \tag{4.14}$$

where

DIC = Direct Interdependency Coefficient

N_{rec} = total number of reactions

$v_{c,k}$ = stoichiometric coefficient of species k

ω_k = rate of reaction of kth reaction, mole/(m^3·sec)

$\delta_{d,k}$ = participation of species d in k^{th} reaction

P_c = production rate of species, mole/(m^3·sec)

C_c = consumption rate of species c, mole/(m^3·sec)

DGREP considers the error propagation process rather than follows the DRG's assumption that every interrelated species is equally important. Hence, the overall path-dependent coefficient, R_{cd} is presented and expressed as:

$$R_{cd} = \max\nolimits_{all\ path\ g}(\prod_{j=1}^{N_{s,g}-1} r_{s_j s_{j+1}}) \qquad (4.15)$$

where

R_{cd} = overall path-dependent coefficient

$N_{s,g}$ = total number of species in path g

r = Direct Interaction Coefficient

$s_j = j^{th}$ species: s_1 is species c and s_{n_s} is species d

Similarly to DRG, elimination of unimportant species is based on the predetermined tolerable error threshold, E_t. Species with $R_{cd} < E_t$ are then removed from the mechanism. In the reduction procedure, DRGEP is applied at first step of reduction.

4.3　　Test Conditions Used for Model Validations and Mechanism Reduction

In mechanism reduction of MCH, predictions accuracy under conditions of JSR and auto-ignition are selected as the criteria instead of auto-ignition conditions only. This is because, it is noted that the reduced models have higher accuracy in predictions of species concentration profiles and ignition delays after data source of JSR conditions are added as demonstrated in the work done by Poon, et al. (2014). Besides, JSR conditions are critical for simulating the extinction process of combustion at steady-state (Cheng, et al., 2015; Poon, et al. 2016a). The operating conditions used for model validations and mechanism reduction of MCH are tabulated in Table 4.1.

Table 4.1: Test Conditions Used for Model Validations and Mechanism Reduction

	Operating Conditions	
	Auto-ignition[a]	JSR[a]
ϕ (-)	0.5, 1.0, 2.0	0.5, 1.0, 2.0
Initial Temperature (K)	650 – 1350 (Interval of 100 K)	650 – 1350 (Interval of 100 K)
Initial Pressure (bar)	40, 60, 80	40, 60, 80
Residence Time[b]	-	1

[a] Operation conditions are chosen according to the conventional in-cylinder pressure values of direct-injection, light-duty diesel engines during the event of fuel injection (Le and Kook, 2015; Poon, et al., 2016a).

[b] Residence time selected in accordance with the minimum time for the extinction process of combustion at steady-state (Cheng, et al., 2015; Poon, et al. 2016a).

4.4   Reduction Procedure via Five-Stage Reduction Scheme

In this section, detail documentation of mechanism reduction and model validations are presented. Mechanism reduction is done by employed the five-stage reduction scheme proposed by Poon, et al. (2013). Each stage of the reductions is presented, from Section 4.4.1 to Section 4.4.5. In addition, model validations are carried throughout each stage of the reductions. Model validations are accomplished by comparing the simulation results of the detailed model and reduced model with respect to their species mole fraction and ID timing predictions for a broad range of operating conditions in 0-D simulations. Operating conditions used for model validations and mechanism reduction are summarised in Table 4.1.

Once the reduced model is successfully generated, it is further validated against experimental results of ID timings in RCM by Weber, et al. (2014) and species moles fraction in JSR by Bissoonauth, et al. (2019). Operating conditions of these experimental results are presented in Section 4.5.

4.4.1 Directed Relation Graph with Error Propagation

The detailed MCH model developed by Weber, et al. (2014) which comprises of 1 540 species and 6 498 reactions is used as the base model for kinetic model reduction.

First and foremost, DRGEP method with Dijkstra's algorithm is employed at the initial step of mechanism reduction of MCH. The chosen target species are CO, CO_2, HCO, HO_2, H_2O_2, H_2, N_2, C_2H_2, C_6H_6 and $C_6H_5CH_3$. CO and CO_2 are the key emission species. HO_2 radical, HCO, H_2O_2 species are vital in chain branching reactions. H_2 are chosen to permit a larger degree of reduction and N_2 is representative of inert species. Besides, C_2H_2 is the precursor species of soot formation. Lastly, C_6H_6 and $C_6H_5CH_3$ are chosen to preserve the aromatic chemistries of the detailed model.

Next, numerical computation of reduction algorithms is done in MATLAB software using the codes of DRGEP method with Dijkstra's algorithm developed by Poon, et al. (2013). In DRGEP reduction, users are prompted to specify the threshold value, E_t that ranging from 0 and 1 to filter the undesirable species. Greater the threshold value, E_t, higher degree of reduction and larger number of species being eliminated as shown in Figure 4.3.
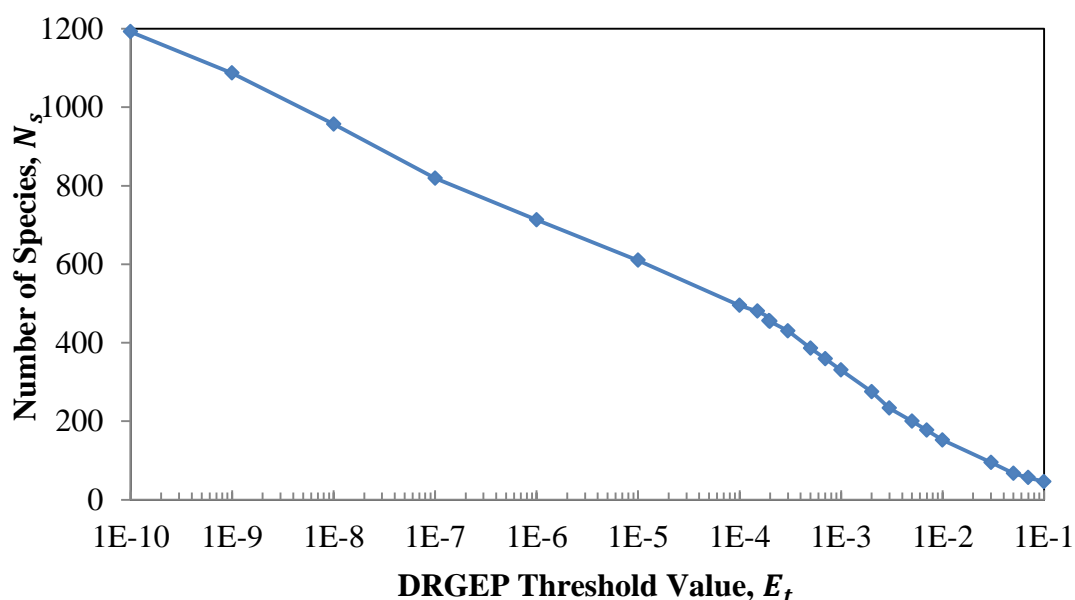
Figure 4.3: Number of Species in Reduced Models Generated from DRGEP Reduction with Different Threshold Value, E_t

Reduced models produced from different threshold values, E_t are then validated by comparing the ID timings with detailed model under auto-ignition conditions. Nevertheless, induced errors in ID timing predictions due to the elimination of species from mechanism are calculated. It is noticed that, the induced error is increased as the threshold value, E_t is increased. It is crucial that the reduced model capable to replicate the combustion properties of the detailed model. Typically, the maximum tolerable deviation for large-scale reduction of mechanism is ranging from 30 % to 50 % (Niemeyer, 2009; Brakora, Ra and Reitz, 2011; Yang, et al., 2012; Luo, et al., 2012). Here, maximum tolerable deviation, D_{MAX} of 50 % is applied.

During the DRGEP reduction procedure, the reduction process is initiated with a threshold value, E_t of 10^{-10}, and then proceed to 10^{-9}, 10^{-8} and so on with increment of the power of ten. As the threshold value, E_t reached 10^{-3}, induced error in ID timings had exceeded the maximum tolerable of 50 % as shown in Figure 4.4. Hence, the elimination test is carried out for species within the range of $10^{-4} \leq E_t \leq 10^{-3}$ and a total of 103 species are involved in the test for precise elimination. Elimination test is started with a threshold value, E_t of 1.0×10^{-4}, and then proceed to 1.2×10^{-4}, 1.4×10^{-4} and so on with increment of 0.2×10^{-4}.
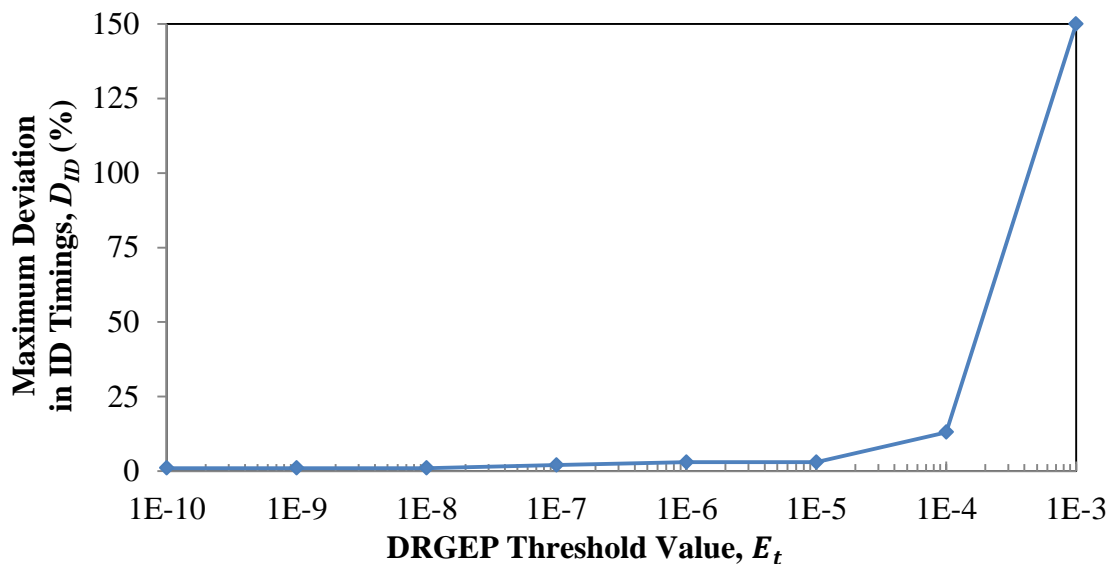
Figure 4.4: Maximum Deviation in ID Timing Predictions that Computed Using Reduced Models Generated from DRGEP Reduction with Different Threshold Value, E_t

During the elimination test, it is found that induced errors have shot up from 8 % to 99 % as the threshold value, E_t increased from 1.8×10^{-4} to 2.0×10^{-4}. This is mainly due to species with threshold value, $E_t > 1.8 \times 10^{-4}$ have significant correlation with the target species. After they are eliminated from the mechanism, remarkable increased in error for ID timing predictions. Nevertheless, threshold value, E_t of 1.8×10^{-4} is chosen as the best E_t to generate a reduced MCH model with 470 species and 2 218 reactions while within the maximum tolerable deviation, D_{MAX} of 50 %.

Comparison of ID timing predictions that computed using both detailed and reduced model is shown in Figure 4.5. It is noticed that the reduced model is able to replicate the ID timing predictions of those of detailed model even though 69 % reduction in number of species, N_s. The computed results of reduced model and detailed model exhibited good agreement for a broad range of operating conditions, and the maximum deviation in ID timings, D_{ID} is only 8 %. Next, comparison of species profiles that computed using both detailed and reduced model is shown in Figure 4.6. The results of species mole fraction predictions are satisfactory. However, the most noticeable deviation is mole fraction predictions of O_2 especially at high temperature region.
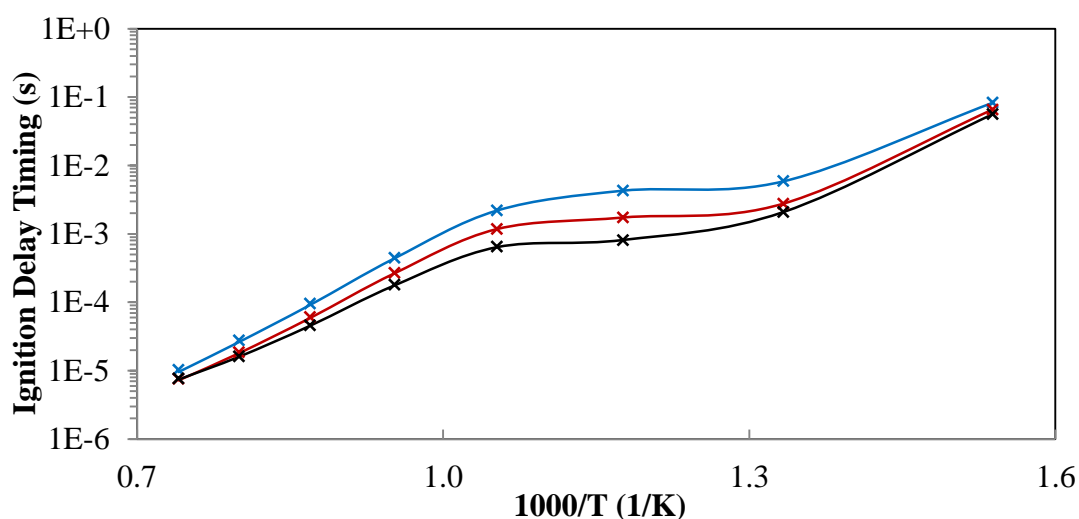
Figure 4.5: Computed ID Timings of MCH Using the Detailed Model (Lines) and Reduced Model (Symbols) for Pressure of 60 bar
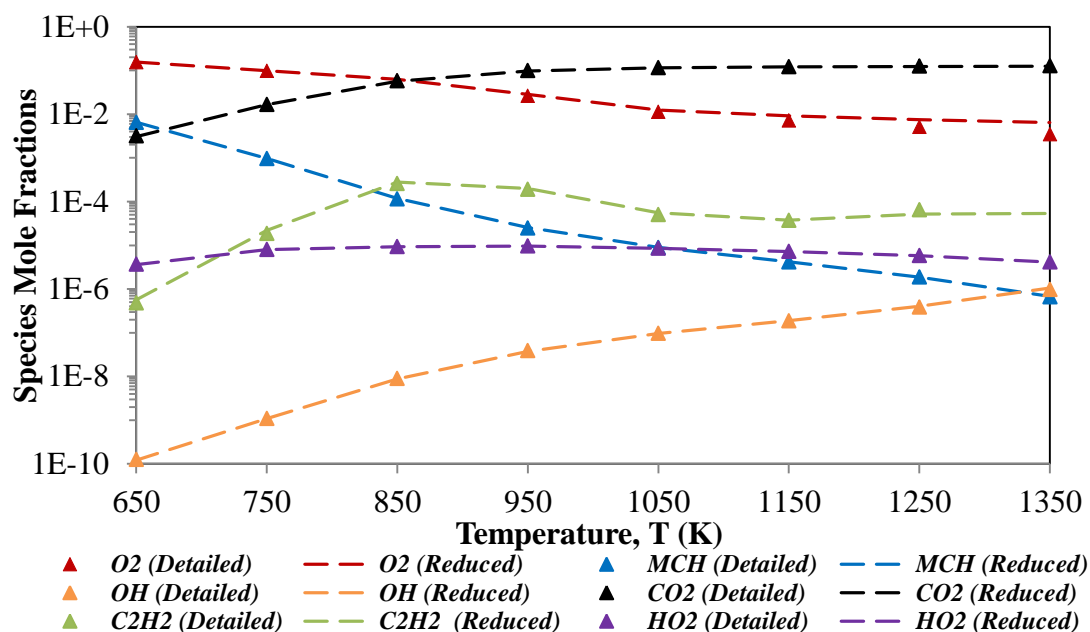
Figure 4.6: Computed Species Profiles under JSR Conditions Using the Detailed Model (Symbols) and Reduced Model (Lines) for Pressure of 60 bar and ϕ of 1.0

4.4.2 Isomer Lumping

Once the reduced MCH model with 470 species and 2 218 reactions was successfully produced using DRGEP method, isomer lumping approach is employed to group isomers existed in the mechanism. Lumping technique is favourable for mechanism with large carbon number owing to the presence of large amount of isomeric species. Besides, the presence of isomers in mechanism may lead to replicated reactions in the mechanism.

Here, isomers are grouped together based on their thermodynamic and transport properties because they usually have similar properties. Hence, their transport equations can be grouped. Isomer lumping approach helps to reduce the complexity of mechanism by substituting reactions of isomers with a representative species. Lumping is a useful method for minimising the size of mechanisms while preserves the important features of original mechanisms (Ra and Reitz, 2008). Isomers present in the reduced model are identified with the aid of the Reaction Pathway Analyser of CHEMKIN-PRO. The major isomer groups of MCH are illustrated in Figure 4.7. Nevertheless, representative isomers are highlighted with red circles. In the Reaction Pathway Analyser, the absolute rates of production for isomers are displayed; representative isomers in each isomer groups are selected on the basis on production rate.
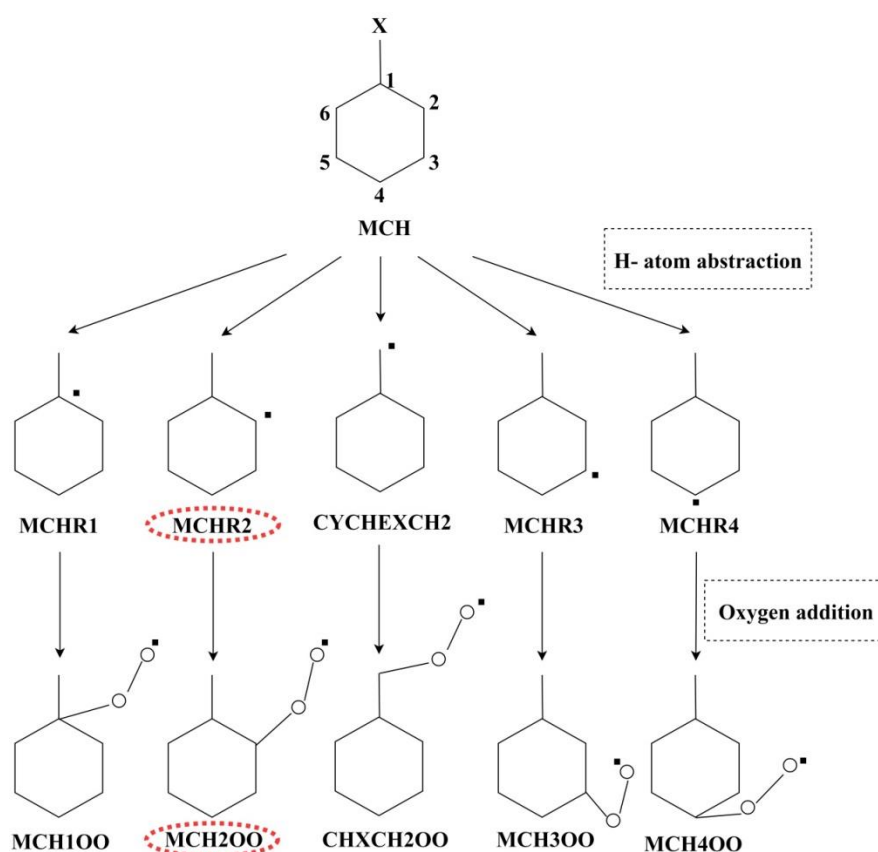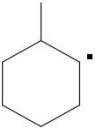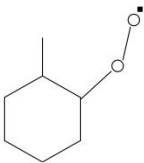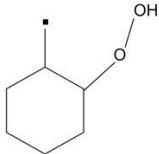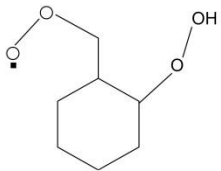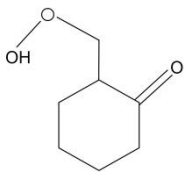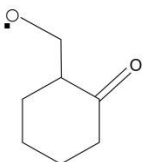
Figure 4.7: Major Isomers Formed During Oxidation of MCH

As illustrated in Figure 4.7, MCH yields 5 alkyl radical isomers (MCHR1, MCHR2, MCHR3, MCHR4 and CYCHEXCH2) through H-atom abstraction processes. Then, alkyl radical isomers are converted to peroxy radical isomers (MCH1OO, MCH2OO, MCH3OO, MCH4OO and CHXCH2OO) through O_2 addition processes.

There are only 5 alkyl radicals formed even though MCH has 7 possible sites (1, 2, 3, 4, 5, 6 and X), this is due to the fact that sites 6 and 5 are equivalent to sites 2 and 3. Reactions of these radical isomers are lumped into the representative reactions. MCHR2 is selected as the representative isomer of alkyl radical isomers while MCH2OO is selected as the representative isomer of peroxy radical isomers due to the highest production rate among its isomer group. Next, isomers with production rate less than 1×10^{-10} mole/(cm^3 · s) are eliminated. Nonetheless, lumped isomers and representative species are tabulated in Table 4.2.

Table 4.2: Selected Representative Species and Lumped Isomers

Representative Species	Structure[a]	Lumped Isomers
MCHR2		MCHR1, MCHR3, MCHR4, CYCHEXCH$_2$
MCH2OO		MCH1OO, MCH3OO, MCH4OO, CHXCH2OO
MCH2QX		MCH2QJ1, MCH2QJ3, MCH2QJ4, MCH2QJ5, MCH2QJ6
MCH2QXQJ		MCH2Q1QJ, MCH2Q4QJ, MCH2Q5QJ, MCH2Q6QJ
MCH2OXQ		MCH2O1Q, MCH2O3Q, MCH2O4Q, MCH2O5Q, MCH2O6Q
MCH2OXOJ		MCH2O1OJ, MCH2O2OJ, MCH2O3OJ, MCH2O5OJ, MCH2O6OJ

[a] Only structures of representative species are shown because structures are similar with those of isomers but radicals and functional groups such as peroxy (ROO), hydroperoxy (ROOH) and carbonyl (=O) are attached to different carbon positions of MCH.

4.4.3 Reaction Path Analysis

Subsequently, Reaction Pathway Analyser of CHEMKIN-PRO is used to study the reaction pathways of MCH oxidation. It is noticed that parallel reaction pathways still exist in the oxidation process of MCH even though isomers were lumped into the representative species.

To further simplify and reduce the mechanism, reactions with normalised temperature sensitivity ($Sen_{normalised}$) less than 0.2 are then eliminated while reactions with higher $Sen_{normalised}$ are retained in mechanism. Removals of species that participated in reactions with low $Sen_{normalised}$ have only little impact on ID timing predictions even if the reactions have high production rates. Equation of $Sen_{normalised}$ is expressed as:

$$Sen_{normalised} = \frac{Sen_i}{Sen_{max}} \qquad (4.16)$$

where

$Sen_{normalised}$ = normalised temperature sensitivity coefficient

Sen_i = temperature A-factor sensitivity for i^{th} reaction

Sen_{max} = maximum temperature A-factor sensitivity among all reactions

For instance, main species that produced from the decomposition of MCH peroxy radical (MCH2OO) are alkene (MCH2ENE), hydroperoxy radical (MCH2QX) and hydroperoxy (MCH2OOH) as illustrated in Figure 4.8. By calculating the normalised temperature sensitivity coefficient of reactions for each individual species, MCH2ENE and MCH2OOH were eliminated owing to relatively low normalised temperature sensitivity coefficient as compared to MCH2QX as shown in Figure 4.9.
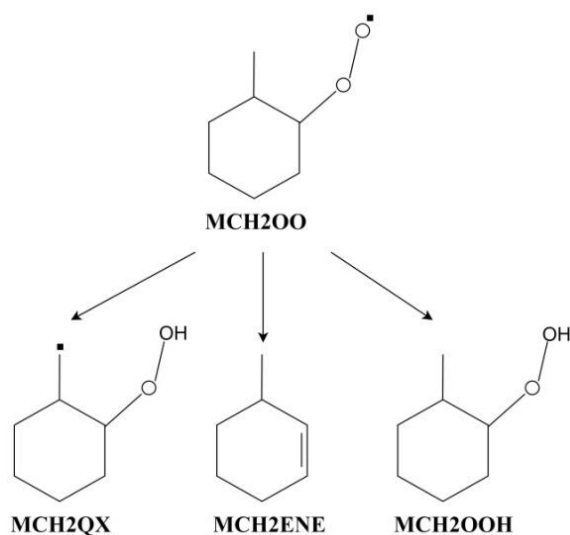
Figure 4.8: Alkene (MCH2ENE), Hydroperoxy Radical (MCH2QX) and Hydroperoxy (MCH2OOH) That Formed From Decompositions of MCH2OO
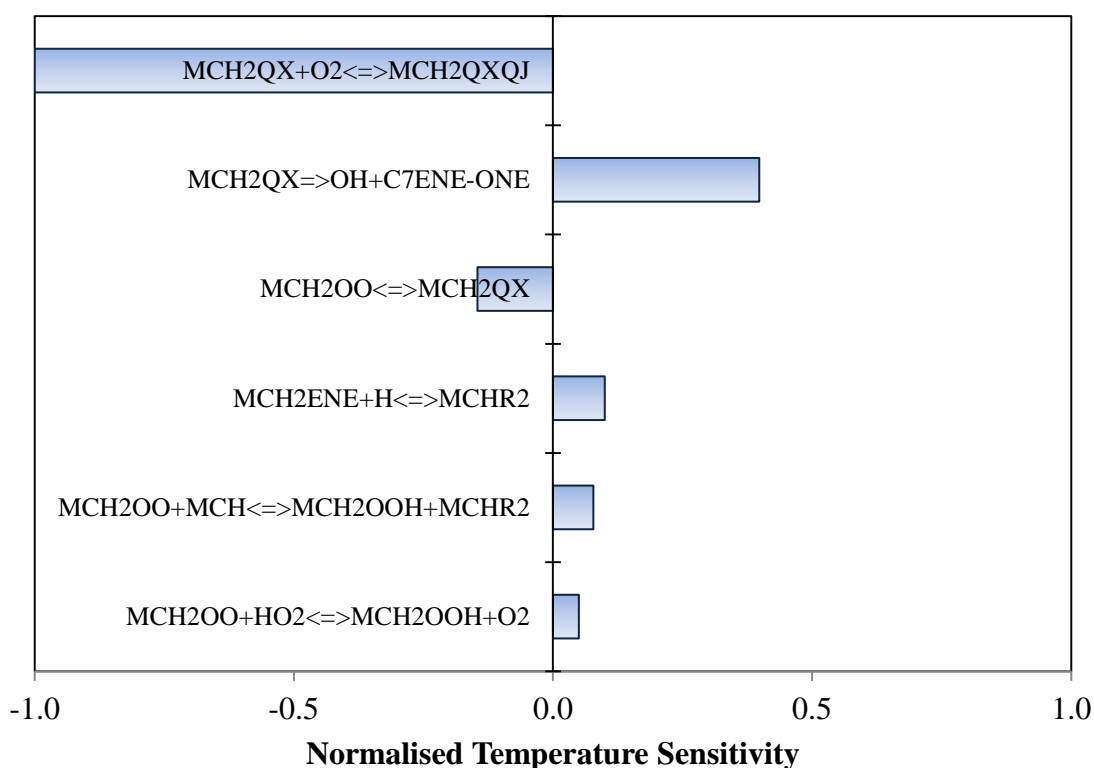
Figure 4.9: Normalised Temperature Sensitivity Chart of MCH for Temperature of 950 K, Pressure of 60 bar and ϕ of 1 [This is a simplified version of normalised temperature sensitivity chart; only normalised temperature sensitivity for reactions of MCH2ENE, MCH2QX and MCH2OOH are shown.]

Fuel decomposition reactions in the reduced model can be categorised 3 types: (1) H-atom abstractions, (2) Thermal uni-molecular decompositions and (3) Ring-opening decompositions as tabulated in Table 4.3. Firstly, H-atom abstractions are the reactions where MCH is attacked by CH_3, C_2H_3, CH_3O, CH_3O_2, O, O_2, OH, HO_2 and H radicals formed MCH radicals. Next, thermal uni-molecular decompositions are the reactions where MCH is decomposed into CHX radical and CH_3. Lastly, ring-opening decompositions are the reactions where cyclic compounds are decomposed into alkenyl radicals.

Table 4.3: Fuel Decomposition Reactions of MCH in the Reduced Model

Types of Fuel Decomposition Reactions

1. H-atom Abstractions

2. Thermal Uni-molecular Decompositions

3. Ring-opening Decompositions

In this MCH mechanism reduction, the ability of reduced model to reproduce the soot formation is concerned apart from the ability to reproduce the combustion characteristics such as ID timings. Hence, subsets of aromatic chemistries are preserved although they have insignificant impact on ID timing predictions. Main reaction pathways that yield toluene are shown in Figure 4.10. Besides, dehydrogenation of MCH directly yields benzene as shown in Figure 4.11.
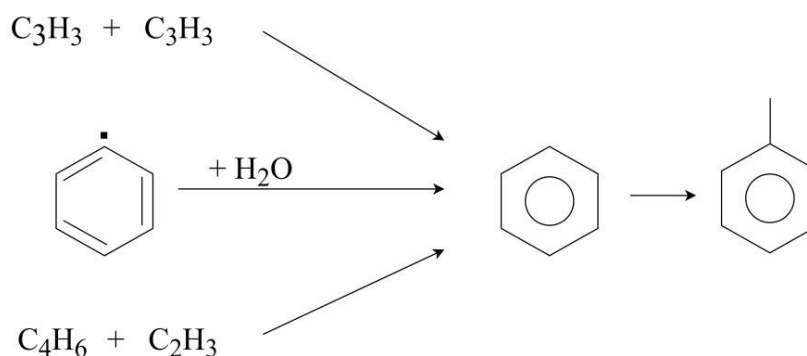
Figure 4.10: Toluene Formation Pathways During Event of Ignition that Computed Using Reduced Model Generated from Isomer Lumping and Reaction Path Analysis for Temperature of 950 K, Pressure of 60 bar and ϕ of 1 [This is a simplified version of reaction pathways that yield toluene; only reactions with high rate of production are shown.]
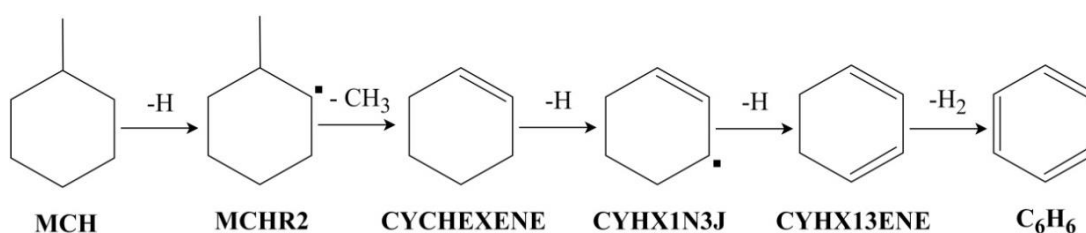
Figure 4.11: Benzene Formation Pathway through Dehydrogenation of MCH

After all the reaction pathways with $Sen_{normalised}$ less than 0.2 were cautiously removed from the mechanism, parallel pathways existed had greatly reduced. Main reaction pathways are simplified to 4 major pathways as illustrated in Figure 4.12. At low temperature, H-atom abstractions on MCH by radicals are prevailing. On the other hand, thermal decomposition of MCH forming CHX radical and CH_3 is dominant at high temperature.
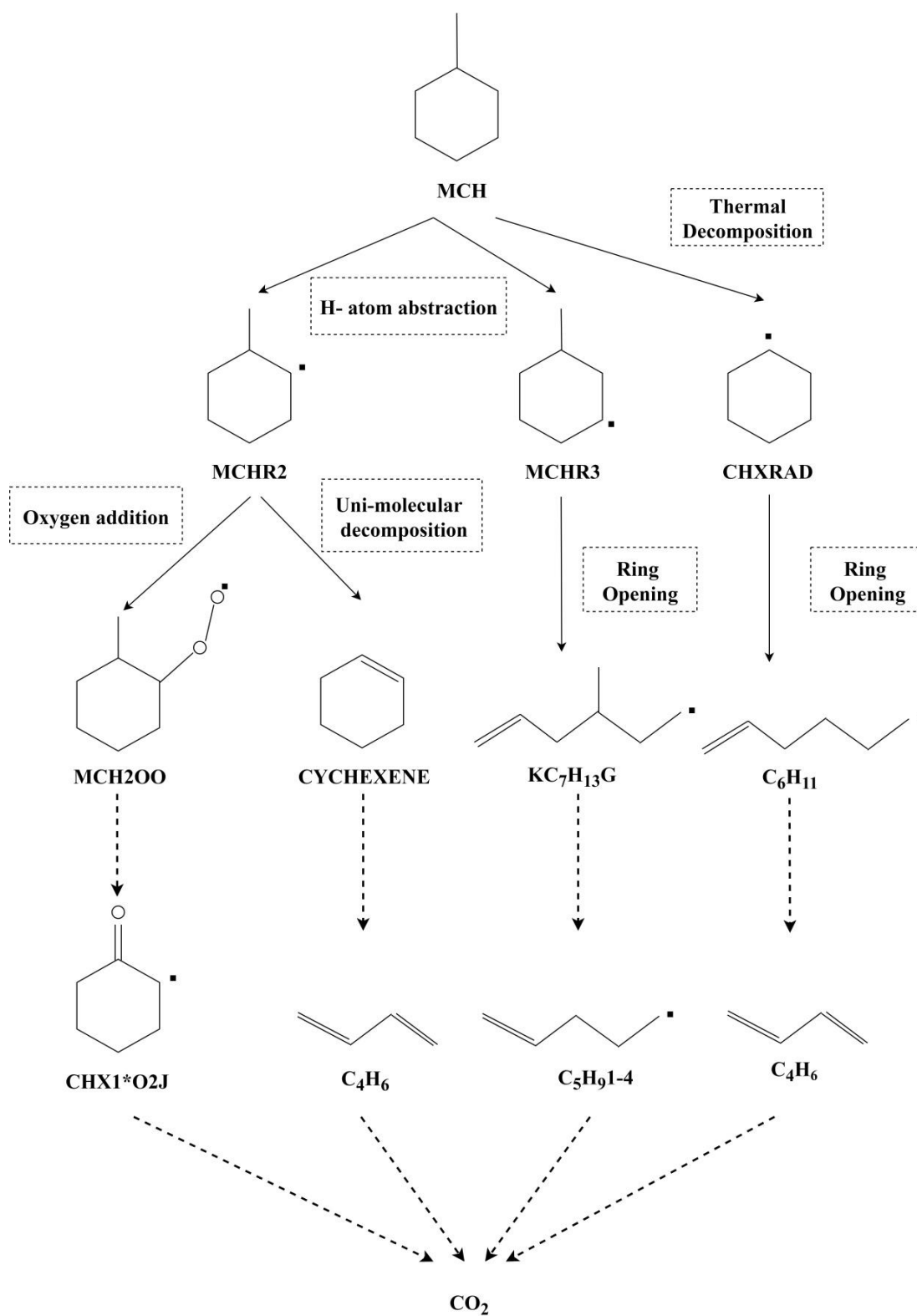
Figure 4.12: Main Reaction Pathways of MCH Oxidation for Pressure of 60 bar, ϕ of 1.0 and Temperature of 650 K, 950 K, 1350 K

4.4.4 Directed Relation Graph

Following that, the DRG mechanism reduction technique is adopted to remove unwanted species that off tracked the reaction paths as the result of isomer lumping and reaction path analysis. In DRG reduction, threshold value, E_t is set to 1 to eliminated unwanted species off tracked the reaction paths. Henceforth, a reduced MCH model with 86 species and 524 reactions was generated. Main reaction pathways are illustrated in Figure 4.13.

Here, a case study is carried out to examine the impacts of eliminating reaction pathways with moderate $Sen_{normalised}$ on the performance of the resulting models. It is aimed to further reduce the mechanism. Hence, reactions associated with species CYCHEXENE and MCHR3 are removed owing to $Sen_{normalised}$ less than 0.5. After removal of reaction pathways with moderate $Sen_{normalised}$, a reduced MCH model with 77 species and 400 reactions was produced. Main reaction pathways are illustrated in Figure 4.14. The abbreviations MCHv1 and MCHv2 are used to represent 86 species mechanism and 77 species reduced MCH mechanism, respectively.
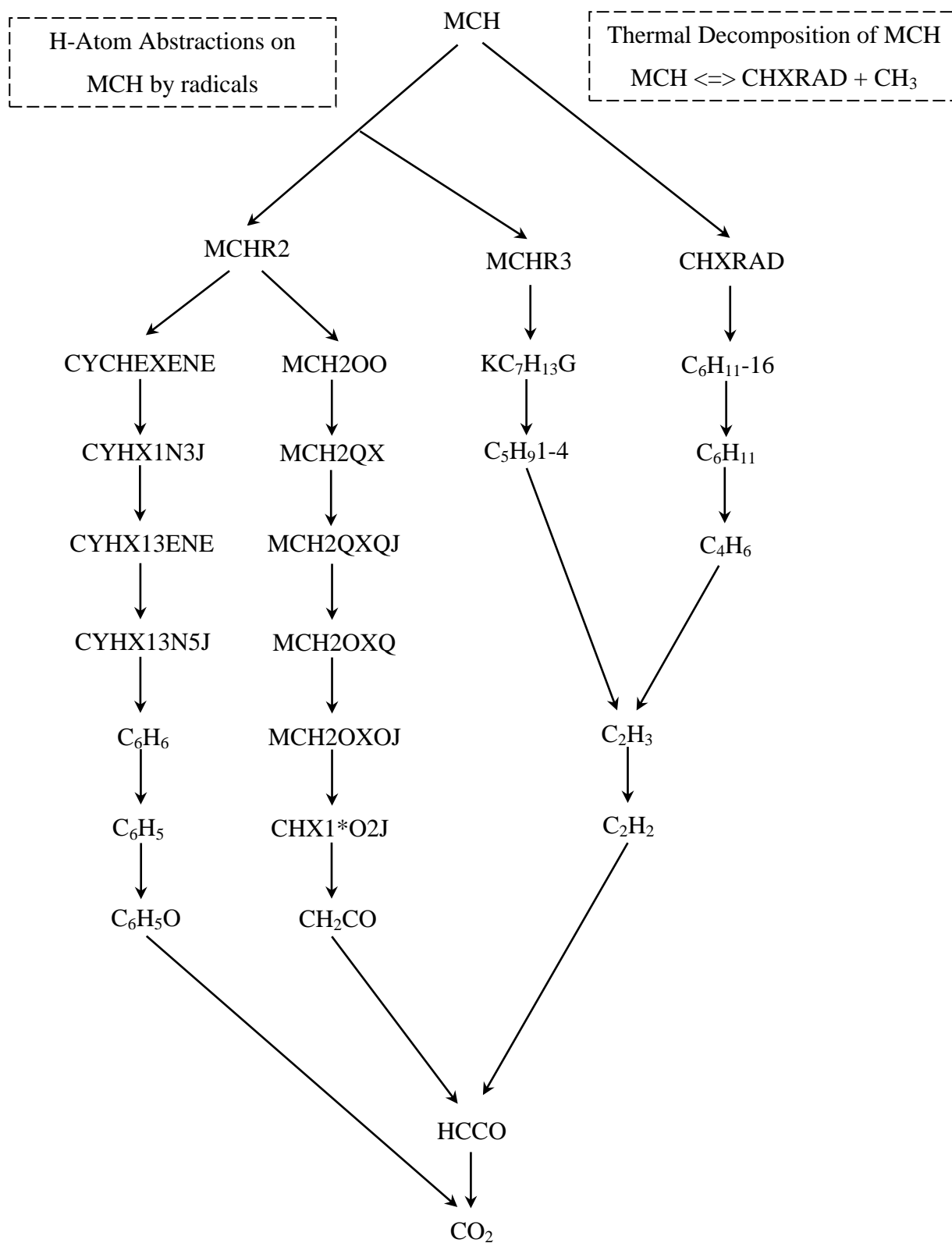
Figure 4.13: Main Reaction Pathways of MCHv1 for Pressure of 60 bar, ϕ of 1.0 and Temperature of 650 K, 950 K, 1350 K

MCH

H-Atom Abstractions on
MCH by radicals

Thermal Decomposition of MCH
MCH <=> CHXRAD + CH$_3$

MCHR2

CHXRAD

MCH2OO

C$_6$H$_{11}$-16

MCH2QX

C$_6$H$_{11}$

MCH2QXQJ

C$_4$H$_6$

MCH2OXQ

C$_2$H$_3$

MCH2OXOJ

C$_2$H$_2$

CHX1*O2J

CH$_2$CO

HCCO

CO$_2$
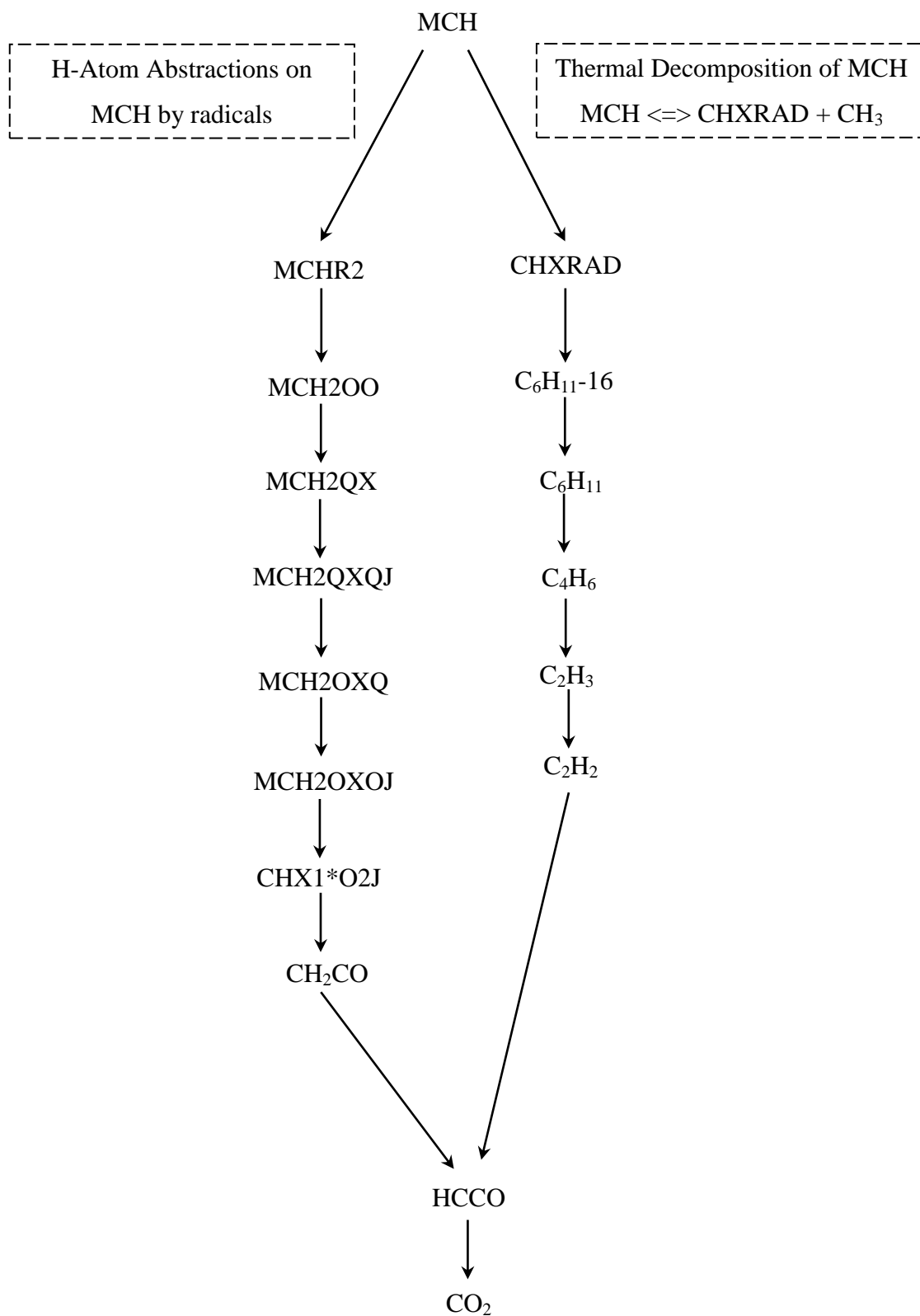
Figure 4.14: Main Reaction Pathways of MCHv2 for Pressure of 60 bar, ϕ of 1.0 and
Temperature of 650 K, 950 K, 1350 K

4.4.5   Adjustment of A-Factor Constant

Once the MCHv1 and MCHv2 reduced MCH mechanisms were successfully generated by using 4 former reduction techniques, deviations in ID timing predictions are large especially in low temperature region and negative temperature coefficient (NTC) region as shown in Figure 4.15. This is due to the reason that the detailed model had experienced about 94 % reduction in number of species. Therefore, sensitivity analysis is conducted on Arrhenius temperature A-factors of elementary reactions. This stage is essential as it helps to optimise the reduced models as well as minimise the induced error in ID timings and species profiles prediction.
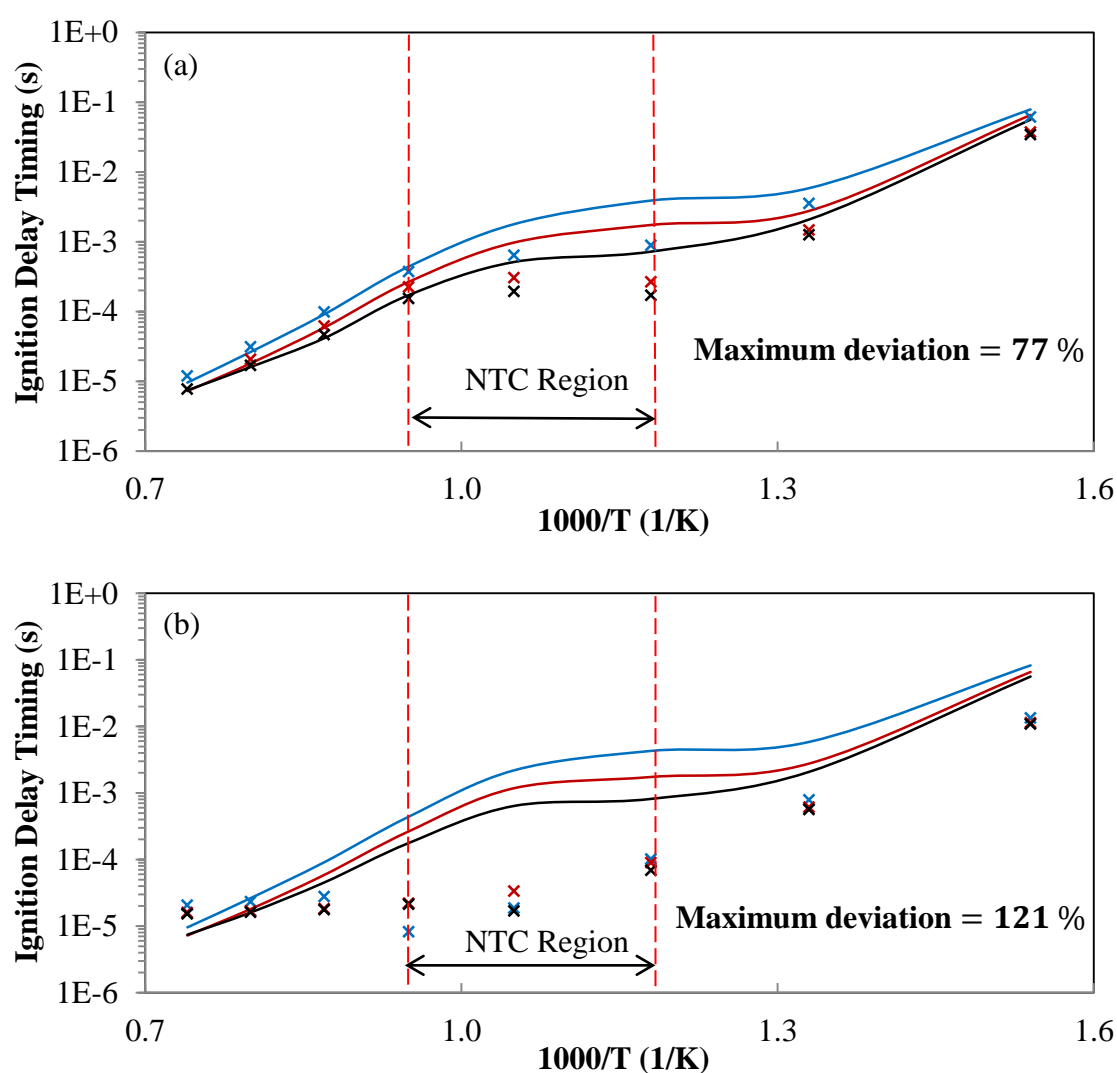
Figure 4.15: ID Timings that Computed Using the Detailed Model (Lines) and Reduced Model (Symbols): (a) MCHv1 (b) MCHv2 Before the Adjustment of A-Factor Constants for ϕ of 0.5 (Blue), 1.0 (Red), 2.0 (Black) and Pressure of 60 bar

Besides, it is noteworthy to mention that isomer lumping reduction technique has contributed to the largest increment in deviation. In isomer lumping, individual group of isomers are lumped into a representative species because they have identical consumption and production reaction pathways. However, single representative species is unable to cope with the consumption and production rate of its isomer group. Hence, the reaction rate constant of the representative species must be adjusted.

As demonstrated by Pepiot and Pitsch (2008) and Narayanaswamy, et al. (2014), isomer lumping reduction followed by tuning in reaction rate constants had minimised the induced errors. Therefore, adjustments of reaction rate constants are conducted on the reactions with high $Sen_{normalised}$ as shown in Figure 4.16. Consequently, it helps to minimise the induced errors so that reduced MCH models comply with the maximum tolerable deviation, D_{MAX} of 50 %.
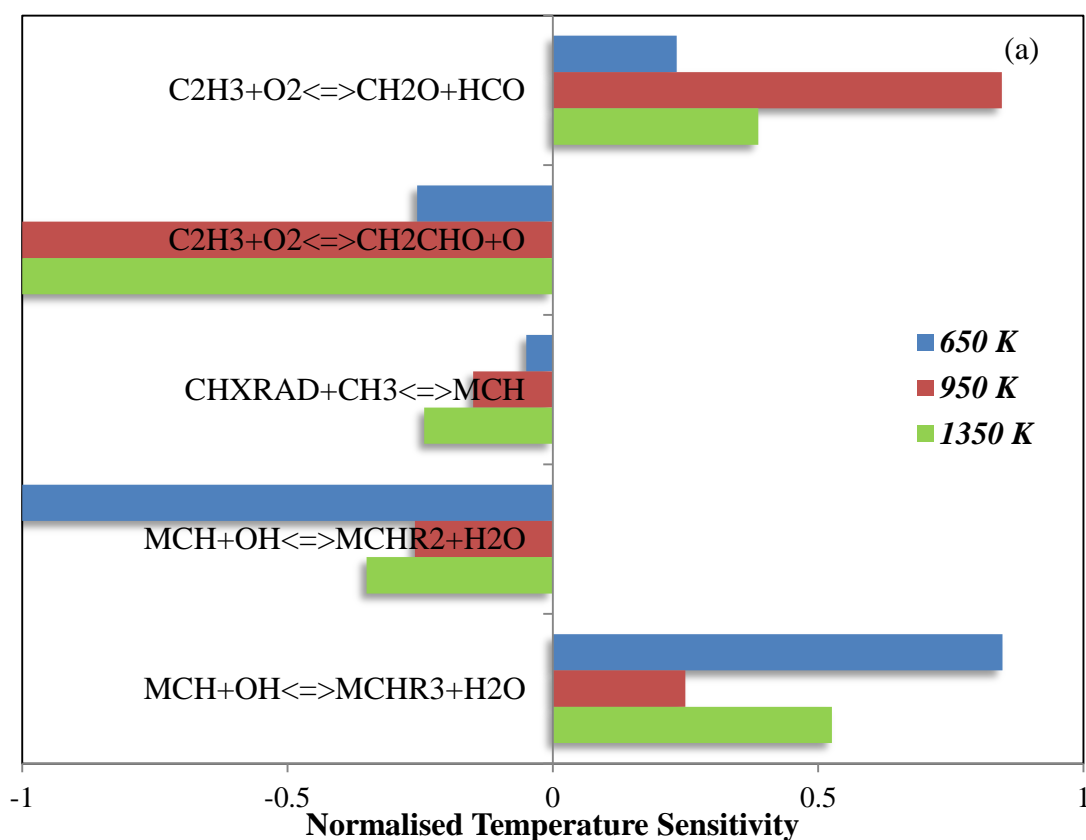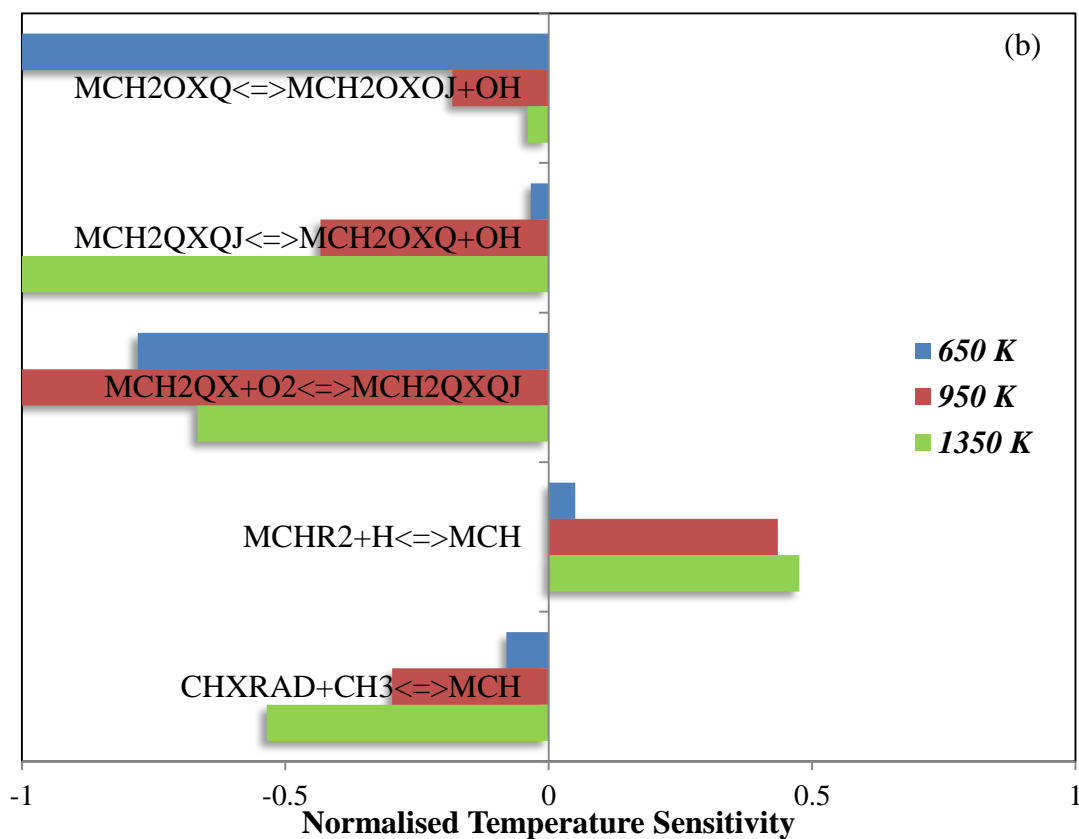
Figure 4.16: Normalised Temperature Sensitivity Chart that Generated Using (a) MCHv1 (b) MCHv2 Before the Adjustment of A-factor Constant for Pressure of 60 bar, ϕ of 1 and Temperature of 650 K (Blue), 950 K (Red) and 1350 K (Green)

As soon as the reactions with high normalised temperature sensitivity are identified, adjustments are made on A-factor of these reactions. Next, the effect of these adjustments on ID timing and species concentration predictions are observed. For MCHv1, it noticed that MCH + OH <=> MCHR2 + H$_2$O has high impact on ID timings at low temperature region while CYCHEXENE + CH$_3$ <=> MCHR2 has great influence on ID timings at NTC region. For MCHv2, it noticed that MCH2OXQ <=> MCH2OXOJ + OH has high impact on ID timings at low temperature region while CHXRAD + CH3 <=> MCH has great influence on ID timings at high temperature region as well as MCH concentration predictions. Therefore, these high sensitivity reactions are finely tuned to give desired effects such as improved ID timings and MCH concentration predictions. By combining these desired effects of adjustments made on selected reactions, reduced models of MCH are then optimised. Reactions that selected for adjustments are summarised in Table 4.4.

Table 4.4: **A**djustments That Made on A-factor Constants of Fuel Species Reactions for (a) MCHv1 (b) MCHv2

Reactions	A-factor Constants	Desired Effects	
		ID Timing[a]	Fuel concentration
(a) MCHv1			
MCH + OH <=> MCHR2 + H_2O	1.95E+5 (Initial) 9.55E+5 (Tuned)	Improvement at high temperature	-
CYCHEXENE + CH_3 <=> MCHR2	1.76E+4 (Initial) 7.76E+4 (Tuned)	Improvement at NTC	-
(b) MCHv2			
CHXRAD + CH_3 <=> MCH	6.63E+14 (Initial) 6.63E+17 (Tuned)	Improvement at high temperature	Improvement in MCH prediction
MCH + O_2 <=> MCHR2+HO_2	4.00E+13 (Initial) 1.40E+15 (Tuned)	Improvement at NTC	-
MCH + OH <=> MCHR2 + H_2O	1.95E+05 (Initial) 1.95E+04 (Tuned)	Improvement at NTC	-
MCH2QX + O_2 <=> MCH2QXQJ	2.00E+12 (Initial) 1.00E+11 (Tuned)	Improvement at low temperature	Improvement in MCH prediction
C_6H_{11}-16 <=> C_6H_{11}	3.67E+12 (Initial) 3.67E+15 (Tuned)	Improvement at high temperature	-

[a] Low Temperature: 650 K – 850 K; NTC: 850 K – 1050 K; High Temperature: 1050 K – 1350 K.

Finally, the reduced MCH models were successfully developed by employing the five-stage reduction scheme proposed by Poon, et al. (2013). The reduced models are validated against detailed model under JSR conditions and auto-ignition conditions in 0-D simulations. These conditions are summarised in Section 4.3. For 0-D simulations using the closed homogeneous batch reactor, results for species moles fraction and ID timing predictions are illustrated in Figure 4.17 and Figure 4.18, respectively.

As illustrated in Figure 4.17, species profiles under auto-ignition conditions are computed using reduced models and detailed model. Species profiles computed using reduced models show similar trends with those of detailed model but shifted to a shorter time. This happened because individual isomer group had substituted into representative species, and the representative species alone is unable to cope with the consumption and production rate of lumped isomers. Nevertheless, species mole fraction predictions by reduced models at steady state are in good agreement with detailed model although the species profiles had shifted to a shorter time. Therefore, overall predictions of the reduced models are satisfactory.

As shown in Figure 4.18, it is noticed that the reduced models are able to replicate the ID timing predictions of those of detailed model even though 94 % reduction in number of species. The computed results of reduced models and detailed model exhibited good agreement for a broad range of operating conditions and the maximum deviation in ID timings, D_{ID} are 28 % and 48 % for MCHv1 and MCHv2, respectively. Maximum deviations of both models are within maximum tolerable deviation, D_{MAX} of 50 %.
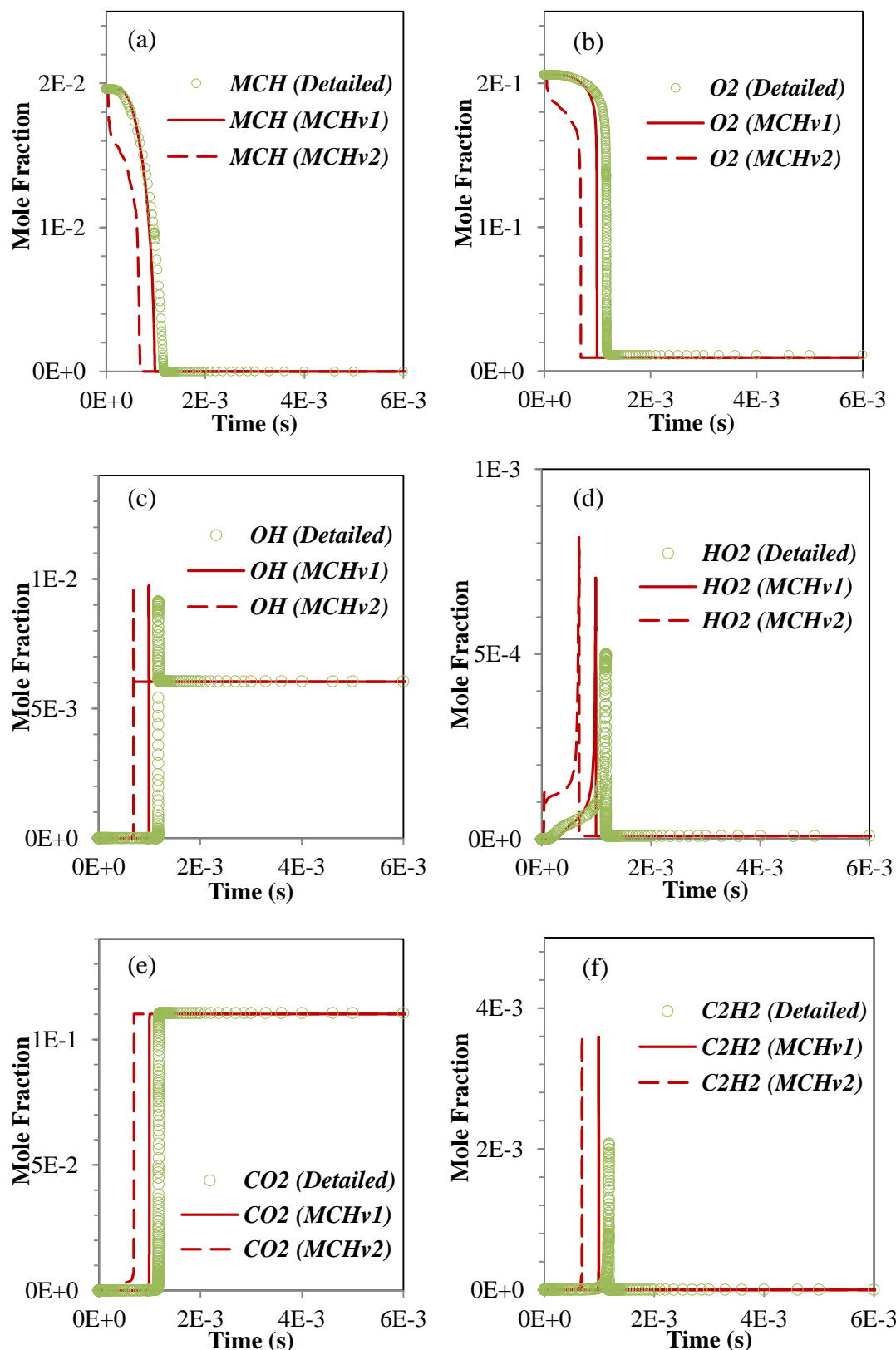
Figure 4.17: Computed Species Mole Fraction Predictions of (a) MCH, (b) O_2, (c) OH, (d) HO_2, (e) CO_2, (f) C_2H_2 Using the Detailed Model (Symbols) and Reduced Models (Lines) for Pressure of 60 bar and ϕ of 1.0
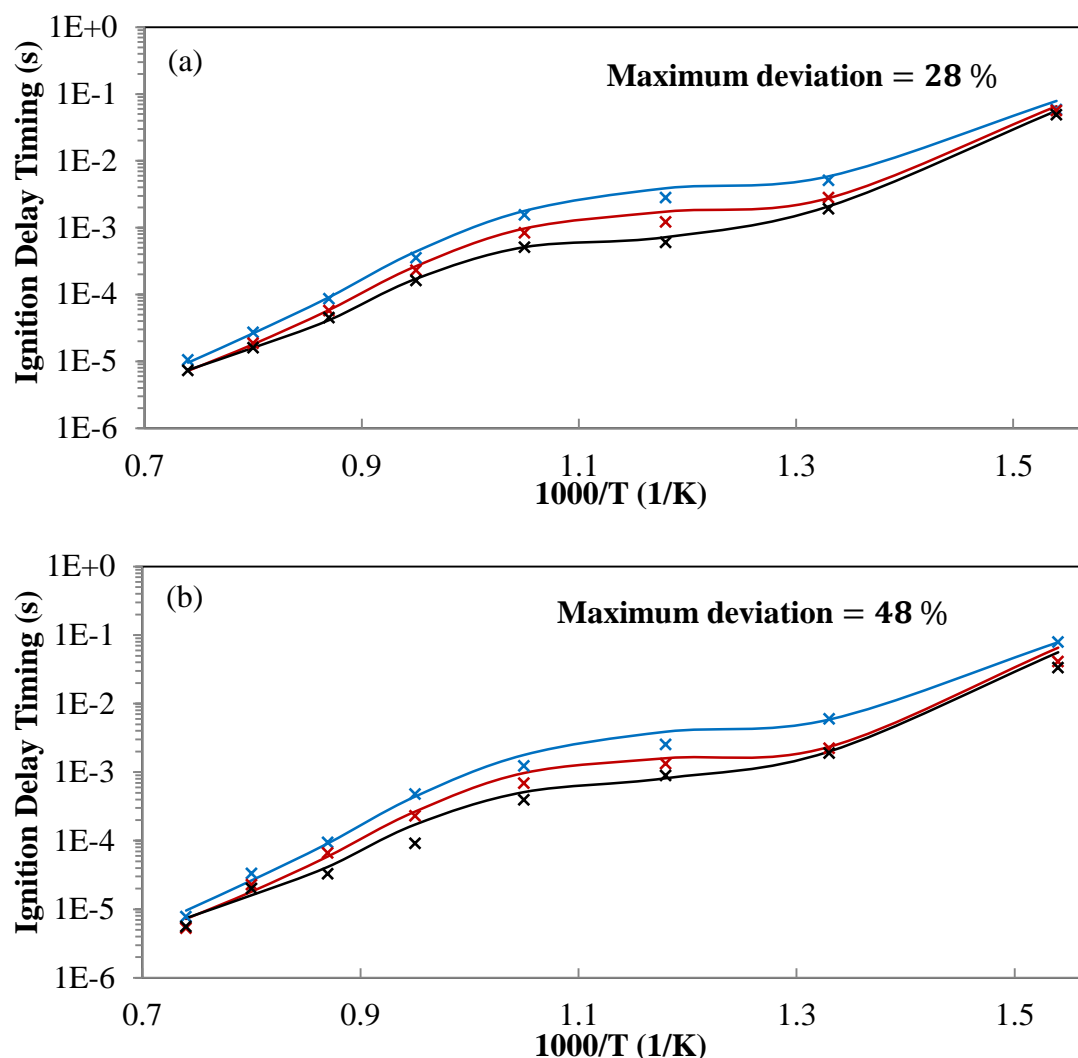
Figure 4.18: Computed ID Timings Using the Detailed Model (Lines) and Reduced Models (Symbols): (a) MCHv1 (b) MCHv2 for ϕ of 0.5 (Blue), 1.0 (Red), 2.0 (Black) and Pressure of 60 bar

For 0-D simulations using PSR reactor, results for species profiles predictions under JSR conditions are shown in Figure 4.19. It is noticed that the reduced models are capable to replicate the species mole concentrations of those of detailed model. However, the computed mole fraction of MCH and C_2H_2 by MCHv2 differ greatly from those of detailed model. In short, computed results of MCHv1 are superior to those of MCHv2 either in auto-ignition or PSR conditions. Hence, MCHv1 is selected as the final reduced model. Lastly, it is acknowledged that the five-stage reduction is efficient for greatly reduce the mechanism of the detailed model. Besides, the compact reduced model developed is able to provide satisfactory results despite simplified chemistry.
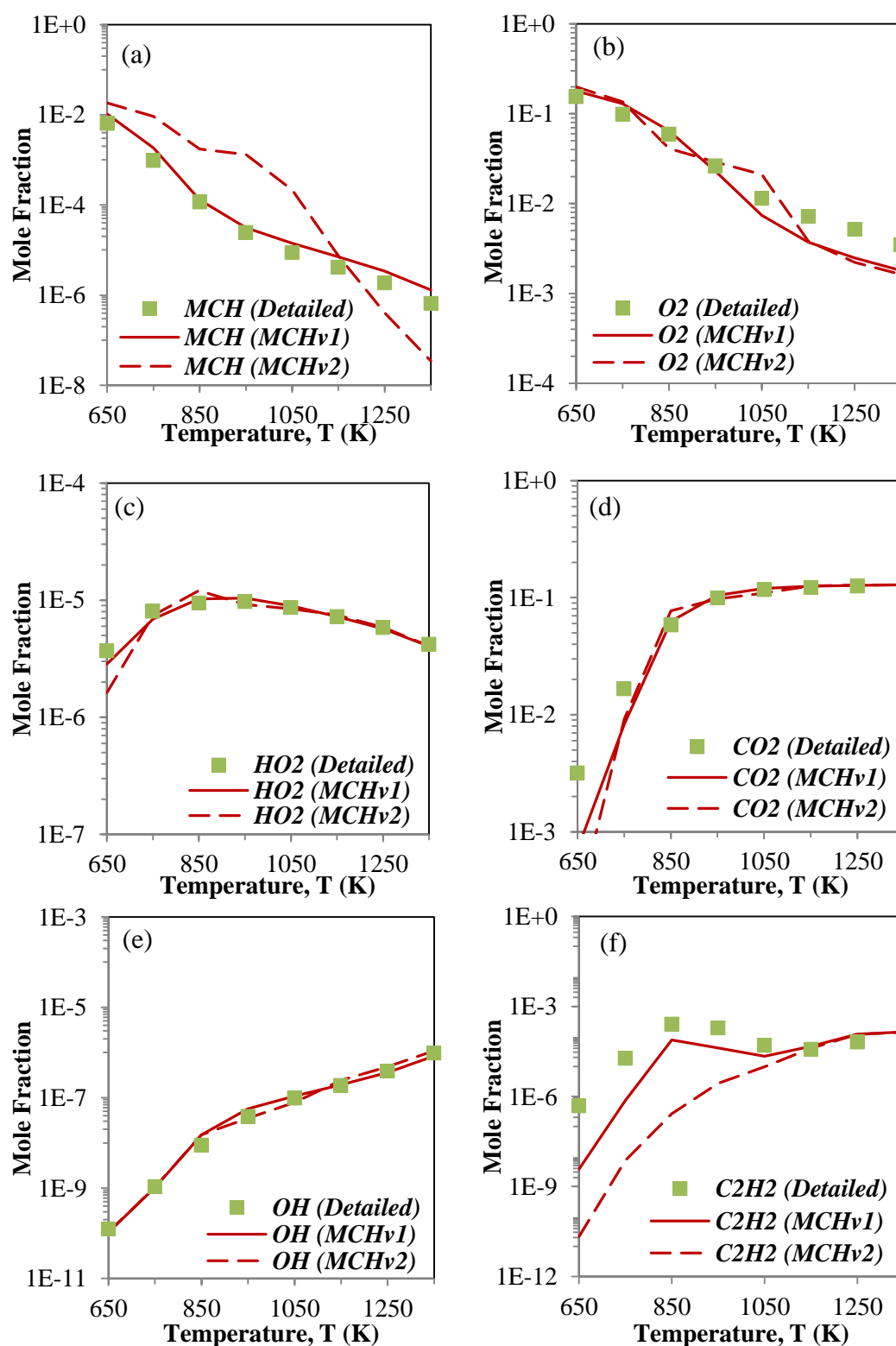
Figure 4.19: Computed Species Mole Fraction of (a) MCH, (b) O_2, (c) HO_2, (d) CO_2, (e) OH, (f) C_2H_2 Using the Detailed Model (Symbols) and Reduced Models (Lines) Under JSR Conditions for Pressure of 60 bar and ϕ of 1.0

4.5 Model Validations against Experimental Results

MCHv1 was chosen as the final reduced model as it has better accuracy in species mole fraction and ID timing predictions. Then, MCHv1 is further validated against experimental results of ID timings under auto-ignition conditions by Weber, et al. (2014) and species moles fraction predictions under JSR conditions by Bissoonauth, et al. (2019). Operating conditions of these experimental results are tabulated in Table 4.5. Comparisons between computed and experimental results for ID timings and species moles fraction are shown in Figure 4.20 and Figure 4.21, respectively.

Table 4.5: Test Conditions Used For Model Reduction and Model Validations against Experimental Results

	Operating Conditions	
	Auto-ignition[a]	JSR[b]
ϕ (-)	0.5, 1.0, 1.5	0.25, 1.0, 2.0
Initial Temperature (K)	650 – 950 (Interval of 50 K)	500 – 1100 (Interval of 100 K)
Initial Pressure (bar)	50	1.067
Residence Time	-	2

[a] Operation conditions are based on the experimental measurements of ID timing for MCH in RCM by Weber, et al. (2014) for model validations.

[b] Operation conditions are based on the experimental measurements of MCH oxidation in JSR by Bissoonauth, et al. (2019) for model validations. Conversion of pressure is from Pa to bar (100 kPa = 1 bar).

As shown in Figure 4.20, MCHv1 is reasonably well in predictions of the actual ignition event. MCHv1 is able to reproduce the ID timings of those of detailed model although 94 % reduction in the size of the mechanism. The computed results and experimental results exhibited good agreement except for the case of equivalence ratio of 1.5. For the equivalence ratio of 1.5, ID timings are under-predicted by the reduced model as well as detailed model. In general, it is observed that ID timing curves computed using the detailed model and reduced model are "s-shaped". Besides, ID timings of MCHv1 are shorter than those of detailed model.
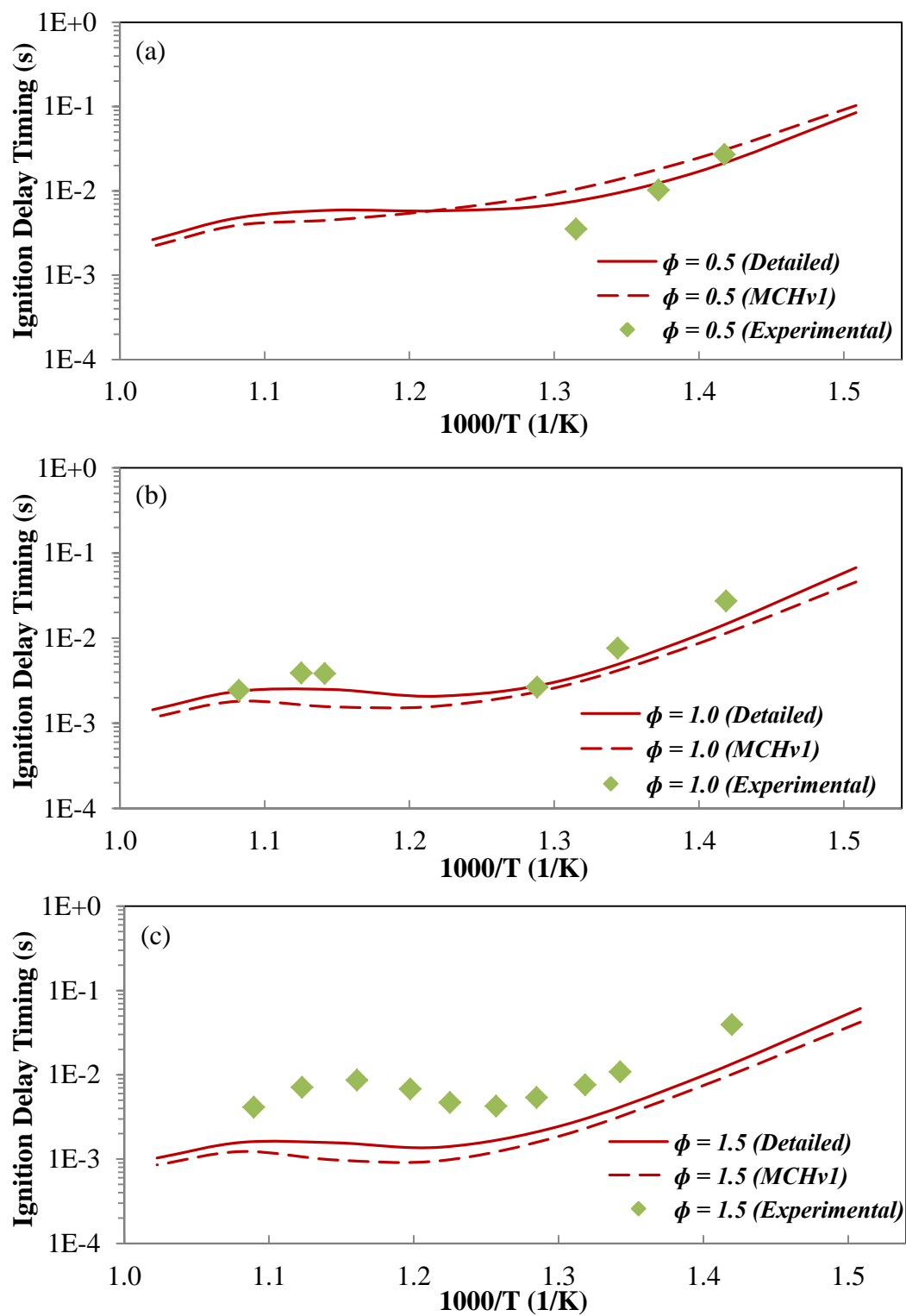
Figure 4.20: Comparisons of ID Timings Between Experimental Data and Computed Results by Detailed and Reduced Models for Pressure of 50 bar and ϕ of (a) 0.5, (b) 1.0, (c) 1.5

Next, MCHv1 is validated against experimental results species moles fraction in JSR as illustrated in Figure 4.21. It is noticed that MCHv1 is able to decently forecast the temporal evolution trends of actual MCH oxidation under JSR conditions. However, there are noticeable deviations in mole fraction concentrations despite overall temporal evolution trends were captured.

Species moles fractions are generally over-predicted by MCHv1 as well as detailed model. In addition, the magnitude of over-predicted in moles fraction is increased as the equivalence ratio is increased. This can be attributed to the reason that the detailed model by Weber, et al. (2014) was originally developed specifically for auto-ignition conditions modelling. Hence, differences between computed and experimental results for species moles fraction under JSR conditions are relatively large as compared to ID timing predictions under auto-ignition conditions.

(a) ϕ of 0.25
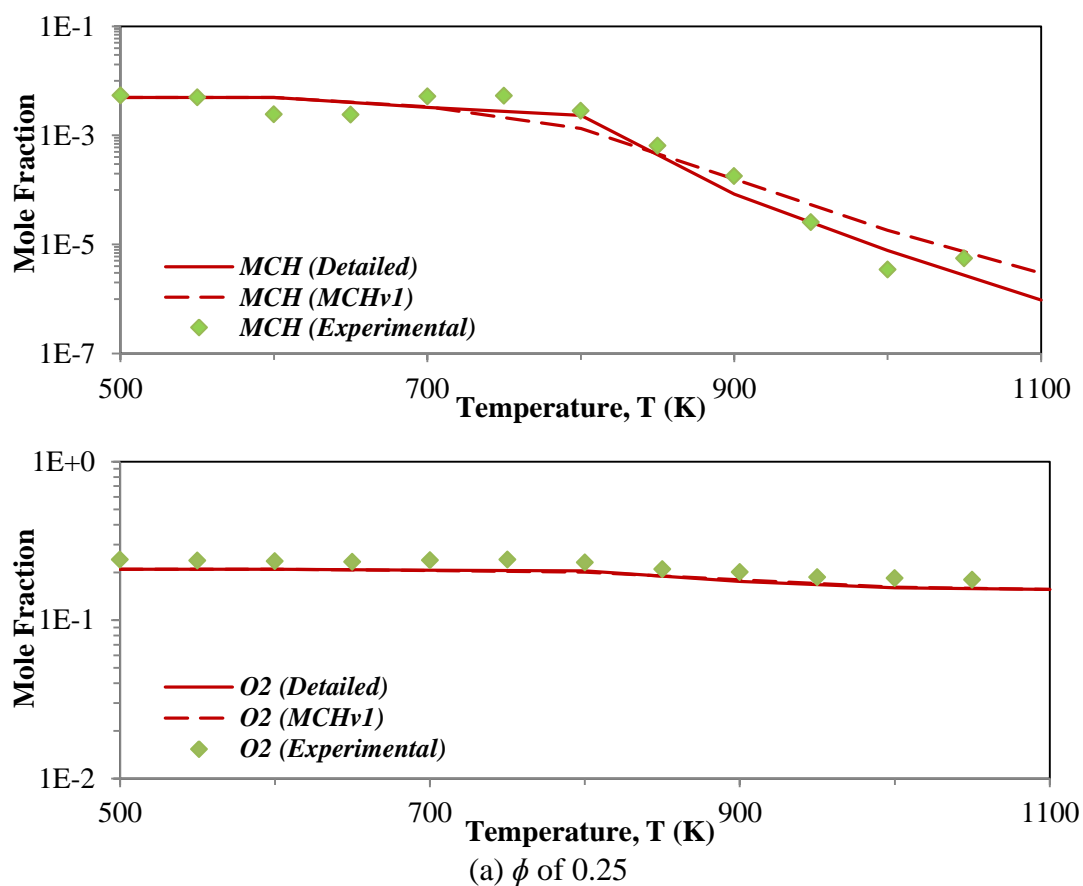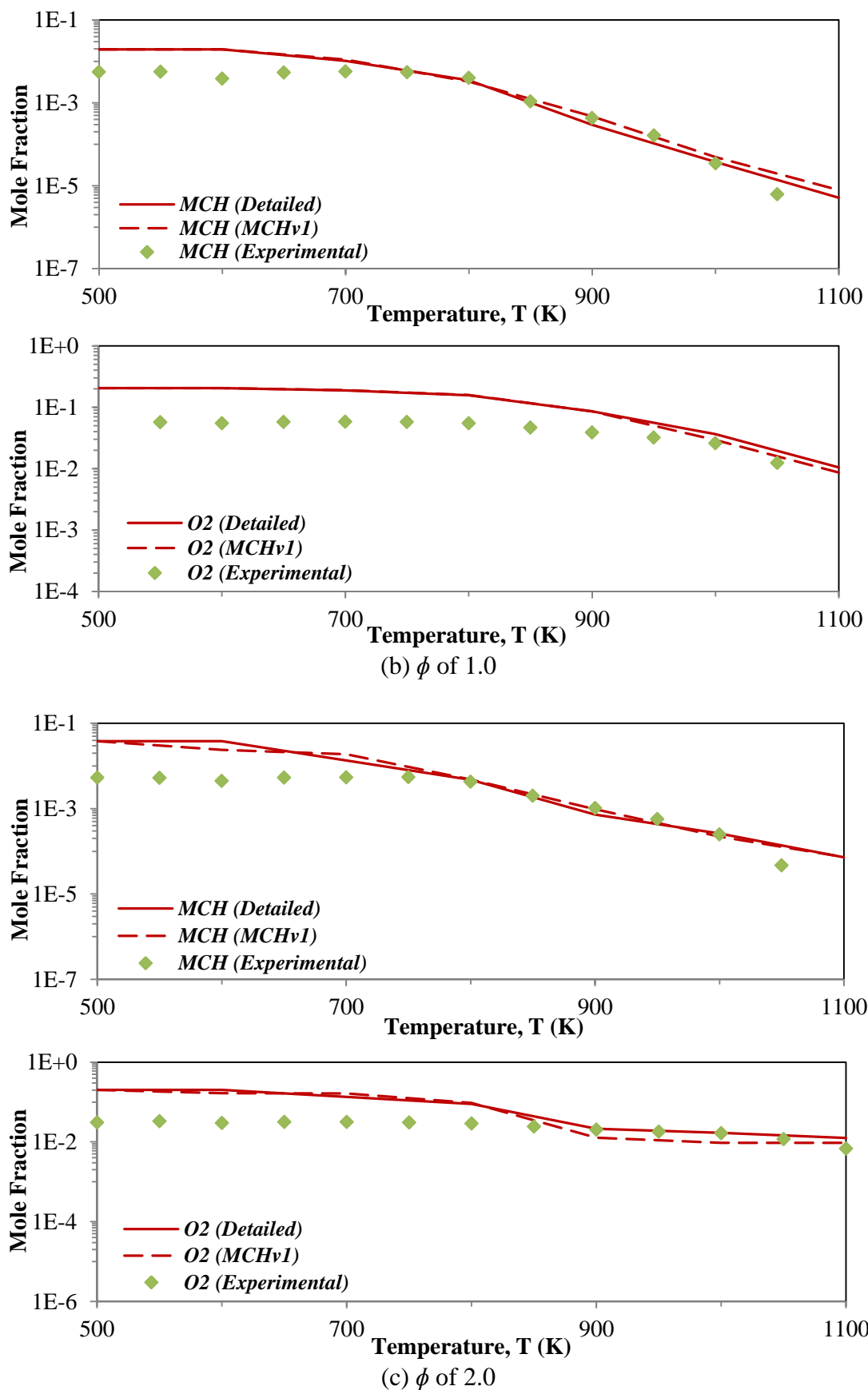
Figure 4.21: Comparisons of Species Profiles between Computed and Experimental under JSR Conditions for Pressure of 1.067 bar and ϕ of (a) 0.25, (b) 1.0, (c) 2.0

4.6   Formulation of a Reduced Diesel Surrogate Fuel Model

In this section, the series of steps in the formulation of a reduced diesel surrogate fuel model is presented. In Section 4.6.1, the base models used to represent each fuel constituent of actual diesel fuels are discussed. In Section 4.6.2, mechanisms merging of the detailed models and reduced models are described. In Section 4.6.3, model validations are presented. The overall flow of reduced diesel surrogate fuel model development is shown in Figure 4.22.

There are 2 common approaches that are widely used: (i) "reduced prior to combination" and (ii) "combined prior to reduction".

(i) "reduced prior to combination" :   The detailed models used to represent each fuel constituent are reduced before combining to form a surrogate fuel model.

(ii) "combined prior to reduction" :   The detailed models used to represent each fuel constituent are combined to form a surrogate fuel model before performing the mechanism reduction.

Here, the "reduced prior to combination" approach is adopted. As demonstrated by Slavinskaya, et al. (2014), Narayanaswamy, et al. (2015) and Poon, et al. (2016a), this approach is able to reduce the complexity of analysis and more computational feasible than reducing the detailed diesel surrogate fuel model. On the other hand, the "combined prior to reduction" approach has higher possibility of truncating or unconsciously repeating the reaction pathways. This is due to the detailed surrogate fuel models have more than 10 000 of reactions.
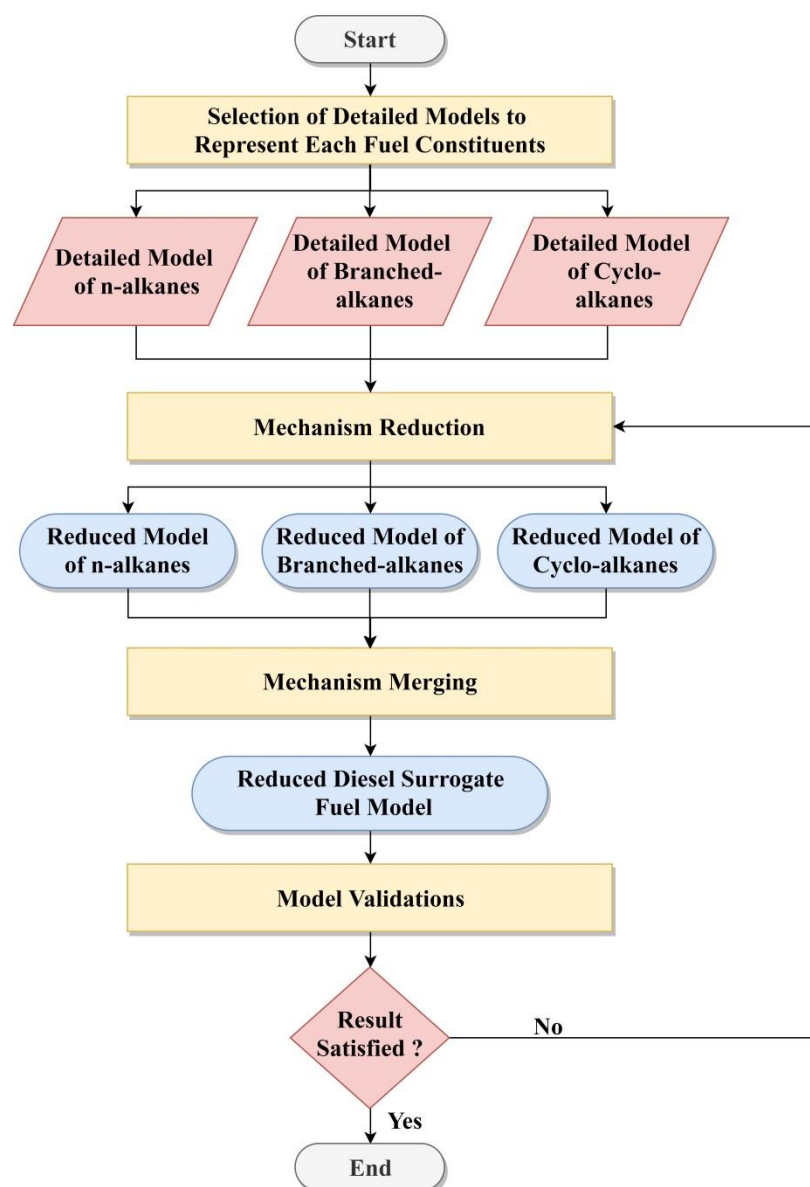
Figure 4.22: Overall Flow of Reduced Diesel Surrogate Fuel Model Development

4.6.1 Representative Models of Fuel Constituents
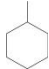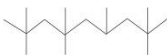
Actual diesel fuels comprise of roughly 25 % aromatic compounds and 75 % aliphatic compounds such as branched-alkanes, n-alkanes and cyclo-alkanes (Huth and Heilos, 2013). In this study, toluene, 2,2,4,4,6,8,8-heptamethylnonane (HMN), n-hexadecane (HXN) and MCH are chosen to represent the aromatic compounds, branched-alkanes, n-alkanes and cyclo-alkanes, respectively. The detailed models of MCH, HMN and HXN proposed by Weber, et al. (2014), Oehlschlaeger, et al. (2009) and Westbrook, et al. (2009), respectively, are used as the base models for the development of reduced diesel surrogate fuel model. Nonetheless, the mechanism of toluene is extracted from sub-mechanism of detailed MCH model.

Firstly, HXN and HMN are the reference fuels for cetane rating of diesel fuels. HXN and HMN are commonly known as n-cetane and iso-cetane, respectively. HXN has CN of 100 while HMN has CN of 15. By blending HXN and HMN with different proportion, different CN can be attained by diesel surrogate fuel model (Oehlschlaeger, et al., 2009; Westbrook, et al., 2009). Next, cyclo-alkanes play an important role in soot formation because they yield aromatic compounds through dehydrogenation. As a consequence, aromatic compounds transform into the PAH which serves as a soot precursor (Sivaramakrishnan and Michael, 2009; Silke, et al., 2007). Hence, more accurate soot formation simulations can be achieved by including cyclo-alkanes in diesel surrogate fuel model. MCH is one of the simplest alkylated cyclo-alkanes, a methyl group attached to 6 carbons cyclo-alkane. In study done by Yang and Boehman (2009), the reactivity of the fuel increased by the methyl group on the ring of cyclo-alkanes. Besides, cyclo-alkanes present in actual diesel fuels are mostly attached to multiple alkyl groups (Wang, 2018). Hence, MCH is a better representative of the cyclo-alkanes than non-alkylated cyclo-alkanes such as CHX. Lastly, toluene is the simplest alkylated aromatic compound, with a methyl group on the benzene ring. Aromatic compounds are abundant in actual diesel fuel, which is about 25 % (Huth and Heilos, 2013). With inclusive of toluene as representative of aromatic compounds, diesel surrogate fuel model has more precise predictions in soot formation.

4.6.2 Mechanism Merging

The reduced HXN model and reduced HMN model developed by Poon, et al. (2016a) are directly applied here to combine with reduced MCH model developed in this study. The details of each reduced model are summarised in Table 4.6.

Table 4.6: Details of Reduced Models that Used in Mechanism Merging

Model	Structure	Number of Species	CN	Hydrocarbon Group
MCH		86	20	Cyclo-alkane
HXN		79	100	N-alkane
HMN		89	15	Branched-alkane

The Advance Mechanism Merger of CHEMKIN-PRO is utilised to merge the mechanisms of reduced HXN, reduced HMN and reduced MCH into a single representative model, namely reduced diesel surrogate fuel model. In mechanism merging, common reactions are identified from mechanisms of reduced HXN, reduced HMN and reduced MCH. It is found that the $C_1 - C_4$ sub-mechanism of MCH is different with those of HXN and HMN. Total of 215 reactions have different rate constants. One example of reaction with different rate constants is reaction H + O_2 <=> O + OH as presented in Figure 4.23. This is because $C_1 - C_4$ sub-mechanism of MCH was developed by Metcalfe, et al. (2013) while $C_1 - C_4$ sub-mechanism of HXN and HMN was developed by Petersen, et al. (2007).

	Mechanism	Written as:	Units	A	B	E	Additional R...	Comment
1	Reduced HXN & HMN	H+O2=O+OH	MOLES CAL/MOLE	1.97E14	0.0	16540.0	REV/1.555E13 0.0E0 4.355E/	none
2	Reduced MCH	h+o2=o+oh	MOLES CAL/MOLE	1.04E14	0.0	15286.0		view (D1)

Figure 4.23: Comparison of Rate Constant between HXN & HMN (Red) and MCH (Blue) for Reaction H + O_2 <=> O + OH [A= pre-exponential factor, (mol · cm · s · K); β= temperature exponent, (-); E_a= activation energy, (cal/mol)]

As demonstrated by Narayanaswamy, et al. (2015), only the most recent set of $C_1 - C_4$ sub-mechanism was kept in merging of 3 mechanisms. It was aimed to avoid duplicated reactions present in the final mechanism. Upon merging, only minor deviations were noticed in simulation results. This procedure is applied here to merge the mechanisms of reduced HXN, reduced HMN and reduced MCH. Hence, $C_1 - C_4$ sub-mechanism of MCH is retained owing to this sub-mechanism is more recent and have been extensively validated. Upon merging, a reduced diesel surrogate fuel model with 144 species and 679 reactions is produced. The abbreviation D_144 is used to represent this model.

4.6.3 Model Validations against Detailed Model

Following that, D-144 is validated against detailed diesel surrogate fuel model with respect to species moles fraction and ID timing predictions under JSR conditions and auto-ignition, respectively. These conditions are summarised in Section 4.3. Results for ID timing and species moles fraction predictions are illustrated in Figure 4.24 and Figure 4.25, respectively.

As shown in Figure 4.24, it is noticed that the D_144 is able to replicate the ID timing predictions of those of detailed model. The computed results of D_144 and detailed model exhibited good agreement for a broad range of operating conditions. Maximum deviation in ID timings, D_{ID} are within the maximum tolerable deviation, D_{MAX} of 50 %. It is observed that only minor deviations in ID timings are induced upon merging.
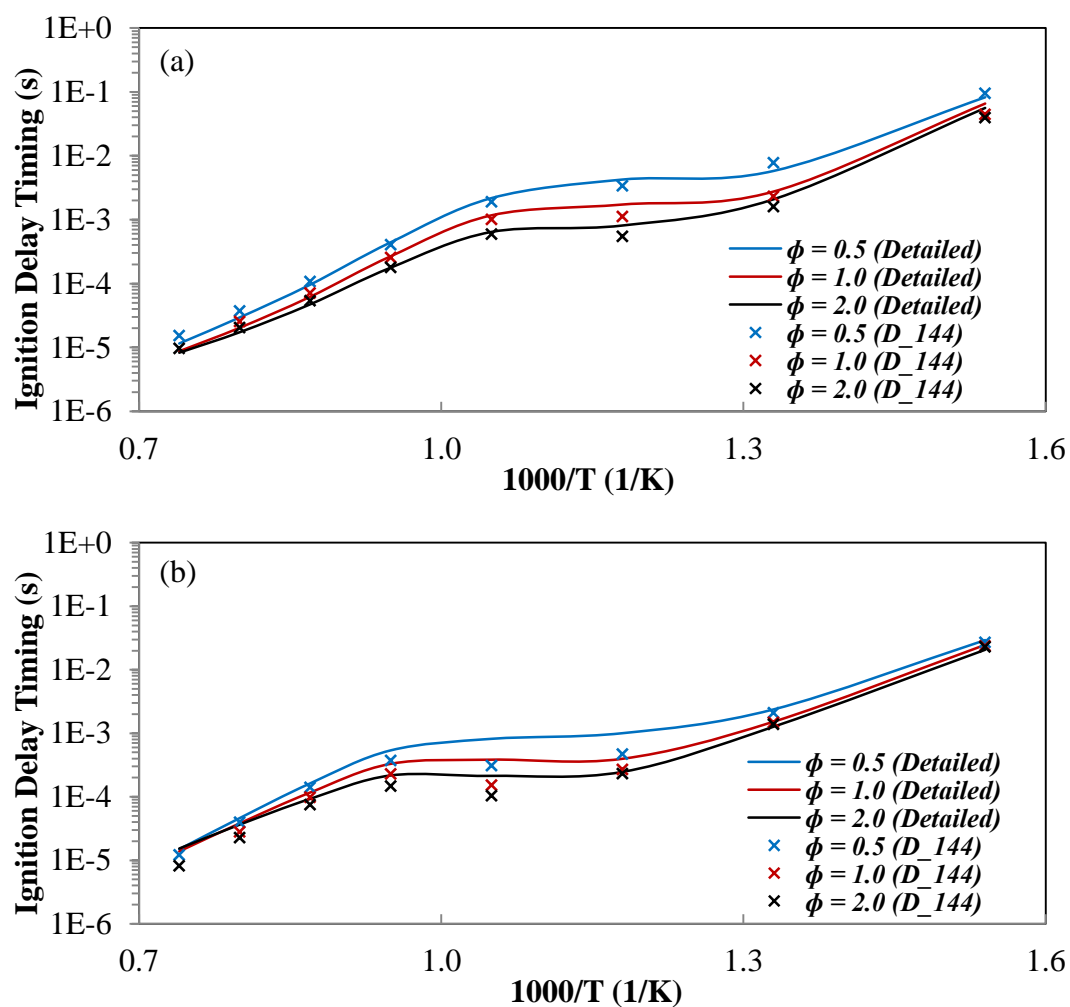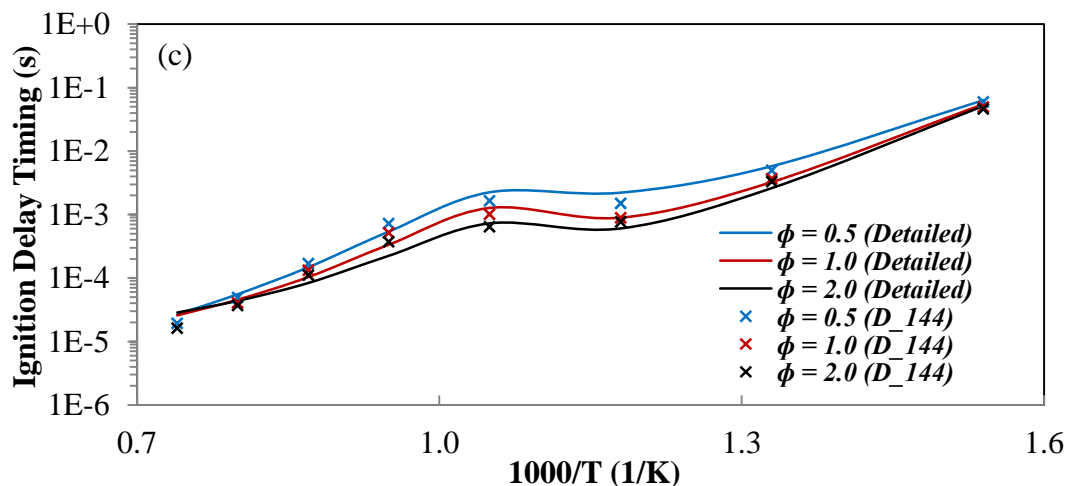
Figure 4.24: Comparisons of Computed ID Timings of Surrogate Components (a) MCH, (b) HXN and (c) HMN Using D_144 (Lines) and Detailed Diesel Surrogate Fuel Model (Symbols) for ϕ of 0.5, 1.0, 1.5 and Pressure of 60 bar

As illustrated in Figure 4.25, species profiles under JSR conditions are computed using D_144 and detailed diesel surrogate fuel model. Species profiles computed using D_144 show similar trends with those of detailed model. However, the noticeable deviations are mole fraction predictions of C_2H_2. Overall, the computed results by D_144 for auto-ignition and JSR conditions are satisfactory.
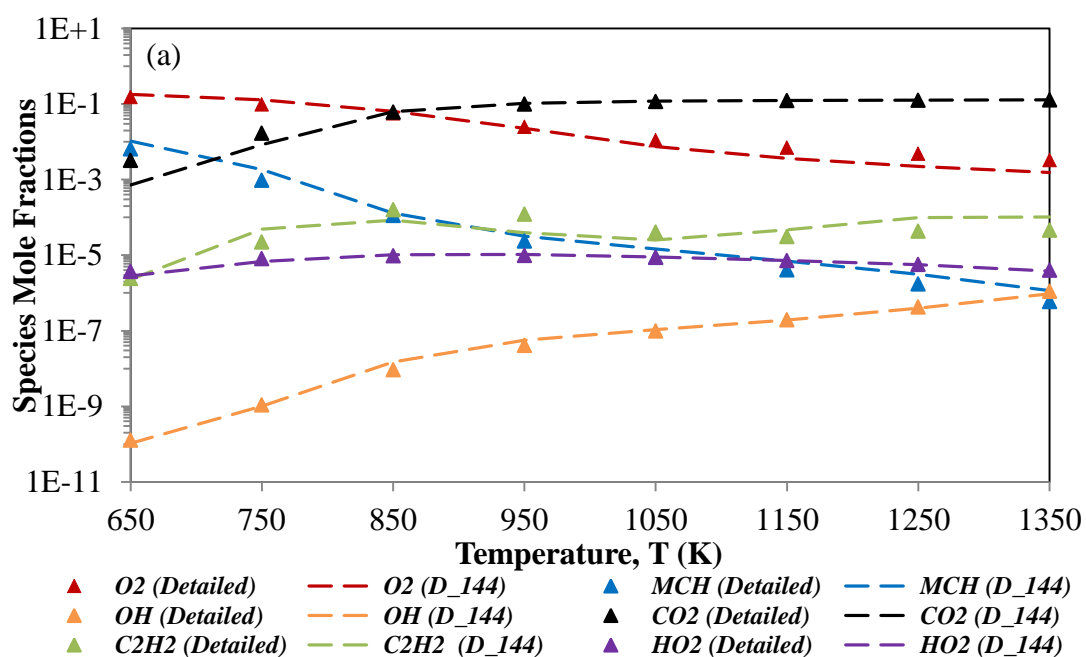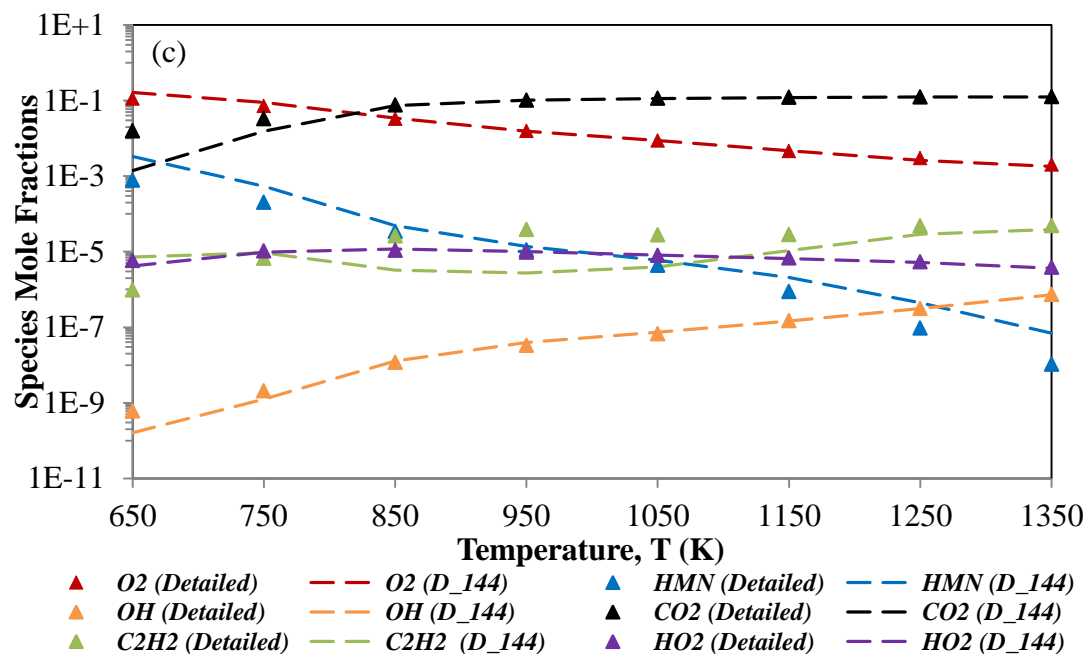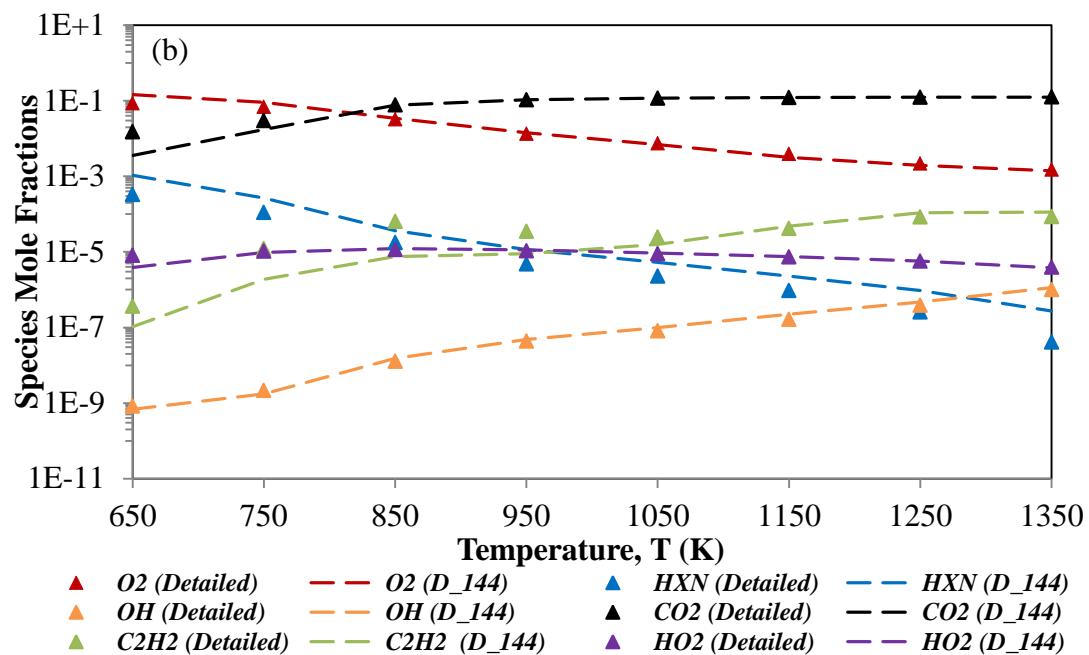
Figure 4.25: Comparisons of Computed Species Profile of Surrogate Components (a) MCH, (b) HXN and (c) HMN Using D_144 (Lines) and Detailed Diesel Surrogate Fuel Model (Symbols) Under JSR Conditions for ϕ of 0.5, 1.0, 1.5 and Pressure of 60 bar

4.7 Summary

In a nutshell, the final reduced MCH model with 86 species namely MCHv1 was successfully produced. Throughout the mechanism reduction, detailed MCH model had experienced 94 % reduction in number of species as shown in Figure 4.26. Nevertheless, a reduced diesel surrogate fuel model was developed by merging the MCHv1 with the reduced HXN model and reduced HMN model developed by Poon, et al. (2016a). Upon merging, a reduced diesel surrogate fuel model with 144 species, namely D_144 was produced.
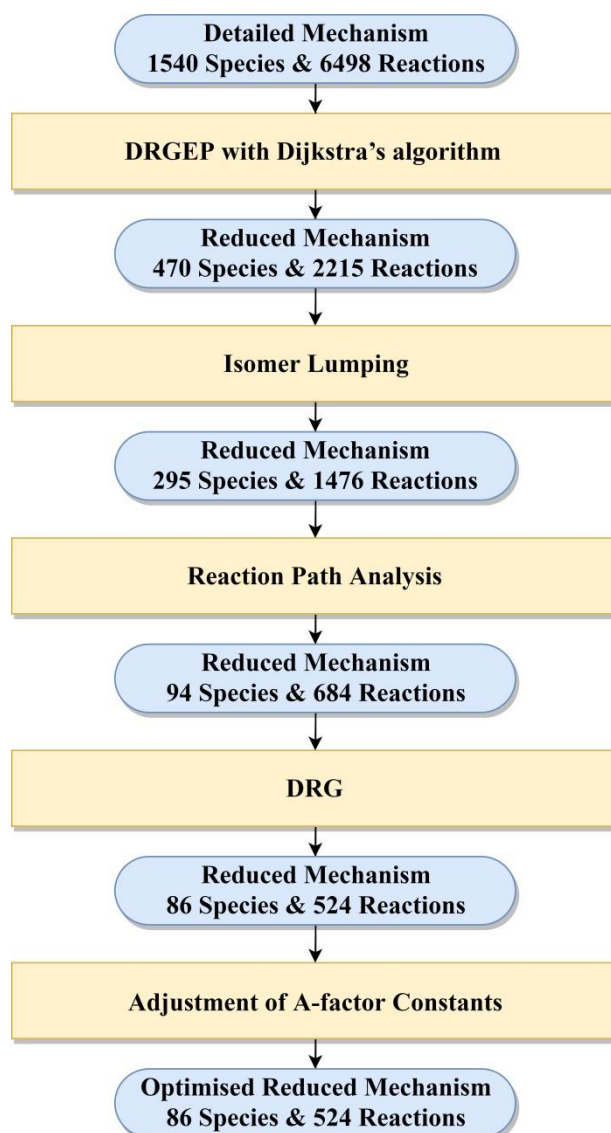
Figure 4.26: Size of Reduced Models in Five-Stage Reduction

CHAPTER 5

CONCLUSIONS AND RECOMMENDATIONS

5.1   Conclusions

In this study, a reduced MCH model with 86 species was successfully produced from the detailed MCH model with 1540 species. The abbreviation MCHv1 was used to represent 86 species reduced MCH model.

MCHv1 was validated against detailed model in 0-D simulations using PSR reactor model and closed homogeneous batch reactor model. Computed results by MCHv1 were in close agreement with the detailed model. Maximum deviation in ID timings, D_{ID} is only 28 %. Following that, the MCHv1 was validated against experimental data of Bissoonauth, et al. (2019) and Weber, et al. (2014) for JSR and auto-ignition conditions, respectively. Computed results under auto-ignition conditions were in close agreement with experimental data. However, noticeable deviations were observed between computed and experimental results for species profiles under JSR conditions. In general, species mole fractions were over-predicted by both MCHv1 and detailed model. This can be attributed to the reason that the detailed model was developed specifically for auto-ignition conditions modelling. Hence, the computed results of the model under JSR conditions are less accurate than auto-ignition conditions.

Lastly, a reduced diesel surrogate fuel model with 144 species, namely D_144 was produced by merging the MCHv1 with reduced HXN model and reduced HMN model developed by Poon, et al. (2016a). D_144 was validated against detailed diesel surrogate fuel model with respect to species moles fraction and ID timing predictions in 0-D simulations. Maximum deviation in ID timings is within maximum tolerable deviation, D_{MAX} of 50 %.

5.2   Recommendations for Future Work

In this study, validations were limited to 0-D simulations using closed homogeneous batch reactor model and PSR reactor model. For the future work, validations in 3-D internal combustion engine simulations and 2-D spray combustion simulations are suggested for better assess the performance of reduced models.

REFERENCES

An, J. and Jiang, Y., 2013. Differences between direct relation graph and error-propagation-based reduction methods for large hydrocarbons. *Procedia Engineering*, 62, pp.342–349.

Bae, C. and Kim, J., 2017. Alternative fuels for internal combustion engines. *Proceedings of the Combustion Institute*, 36(3), pp.3389–3413.

Bakali, A., Braun-Unkhoff, M., Dagaut, P., Frank, P. and Cathonnet, M., 2000. Detailed kinetic reaction mechanism for cyclohexane oxidation at pressure up to ten atmospheres. *Proceedings of the Combustion Institute*, 28(2), pp.1631–1638.

Bhattacharjee, B., Schwer, D.A., Barton, P.I. and Green, W.H., 2003. Optimally-reduced kinetic models: reaction elimination in large-scale kinetic mechanisms. *Combustion and Flame*, 135(3), pp.191-208.

Bissoonauth, T., Wang, Z., Mohamed, S.Y., Wang, J.Y., Chen, B., Rodriguez, A., Frottier, O., Zhang, X., Zhang, Y., Cao, C. and Yang, J., 2019. Methylcyclohexane pyrolysis and oxidation in a jet-stirred reactor. *Proceedings of the Combustion Institute*, 37(1), pp.409-417.

Brakora, J.L., Ra, Y. and Reitz, R.D., 2011. Combustion model for biodiesel-fueled engine simulations using realistic chemistry and physical properties. *SAE International Journal of Engines*, *4*(1).

Buda, F., Heyberger, B., Fournet, R., Glaude, P.A., Warth, V. and and Battin-Leclerc*, F., 2006. Modeling of the Gas-Phase Oxidation of Cyclohexane. *Energy Fuels*, 20(4), pp 1450–1459.

Cavallotti, C., Rota, R., Faravelli, T. and Ranzi, E., 2007. Ab initio evaluation of primary cyclo-hexane oxidation reaction rates. *Proceedings of the Combustion Institute*, 31(1), pp.201-209.

Chang, Y., Jia, M., Li, Y., Liu, Y., Xie, M., Wang, H. and Reitz, R.D., 2014. Development of a skeletal mechanism for diesel surrogate fuel by using a decoupling methodology. *Combustion and Flame*, 162(10), pp.3785–3802.

Chen, J.Y., 1988. A general procedure for constructing reduced reaction mechanisms with given independent relations. *Combustion Science and Technology*, 57(1-3), pp.89-94.

Chen, Y. and Chen, J.Y., 2016. Application of Jacobian defined direct interaction coefficient in DRGEP-based chemical mechanism reduction methods using different graph search algorithms. *Combustion and Flame*, 174, pp.77–84.

Cheng, X., Ng, H.K., Gan, S., Ho, J.H. and Pang, K.M., 2015. Development and validation of a generic reduced chemical kinetic mechanism for CFD spray combustion modelling of biodiesel fuels. *Combustion and Flame*, *162*(6), pp.2354-2370.

Curran, H.J., Gaffuri, P., Pitz, W.J. and Westbrook, C.K., 2002. A comprehensive modeling study of iso-octane oxidation. *Combustion and Flame*, 129(3), pp.253–280.

Dayma, G., Glaude, P.A., Fournet, R. and Battin-Leclerc, F., 2003. Experimental and modeling study of the oxidation of cyclohexene. *International Journal of Chemical Kinetics*, 35(7), pp.273–285.

Debia, M., Couture, C., Njanga, P.E., Neesham-Grenon, E., Lachapelle, G., Coulombe, H., Hallé, S. and Aubin, S., 2017. Diesel engine exhaust exposures in two underground mines. *International Journal of Mining Science and Technology*, *27*(4), pp.641-645.

Edwards, T. and Maurice, L.Q., 2001. Surrogate Mixtures to Represent Complex Aviation and Rocket Fuels. *Journal of Propulsion and Power*, 17(2), pp.461–466.

Edwards, T., Colket, M., Cernansky, N., Dryer, F., Egolfopoulos, F., Friend, D., Law, E., Lenhert, D., Lindstedt, P., Pitsch, H. and Sarofim, A., 2007. Development of an experimental database and kinetic models for surrogate jet fuels. In *45th AIAA Aerospace Sciences Meeting and Exhibit.*

Farrell, J.T., Cernansky, N.P., Dryer, F.L., Law, C.K., Friend, D.G., Hergart, C.A., McDavid, R.M., Patel, A.K., Mueller, C.J. and Pitsch, H., 2007. *Development of an experimental database and kinetic models for surrogate diesel fuels*. SAE Technical Paper.

Fernandes, R.X., Zádor, J., Jusinski, L.E., Miller, J.A. and Taatjes, C.A., 2009. Formally direct pathways and low-temperature chain branching in hydrocarbon autoignition: the cyclohexyl+ O 2 reaction at high pressure. *Physical Chemistry Chemical Physics*, 11(9), pp.1320-1327.

Frassoldati, A., D'Errico, G., Lucchini, T., Stagni, A., Cuoci, A., Faravelli, T., Onorati, A. and Ranzi, E., 2015. Reduced kinetic mechanisms of diesel fuel surrogate for engine CFD simulations. *Combustion and Flame*, 162(10), pp.3991–4007.

Gao, X., Yang, S. and Sun, W., 2016. A global pathway selection algorithm for the reduction of detailed chemical kinetic mechanisms. *Combustion and Flame*, 167, pp.238–247.

Gong, C., Liu, F., Sun, J. and Wang, K., 2016. Effect of compression ratio on performance and emissions of a stratified-charge DISI (direct injection spark ignition) methanol engine. *Energy*, 96, pp.166–175.

Granata, S., Faravelli, T. and Ranzi, E., 2003. A wide range kinetic modeling study of the pyrolysis and combustion of naphthenes. *Combustion and Flame*, 132(3), pp.533–544.

Hariram, V. and Shangar, R.V., 2015. Influence of compression ratio on combustion and performance characteristics of direct injection compression ignition engine. *Alexandria Engineering Journal*, 54(4), pp.807–814.

Herbinet, O., Pitz, W.J. and Westbrook, C.K., 2008. Detailed chemical kinetic oxidation mechanism for a biodiesel surrogate. *Combustion and Flame*, 154(3), pp.507–528.

Hernández, J.J., Sanz-Argent, J. and Monedero-Villalba, E., 2014. A reduced chemical kinetic mechanism of a diesel fuel surrogate (n-heptane/toluene) for HCCI combustion modelling. *Fuel*, 133, pp.283–291.

Huth, M. and Heilos, A., 2013. Fuel flexibility in gas turbine systems: Impact on burner design and performance. *Modern Gas Turbine Systems: High Efficiency, Low Emission, Fuel Flexible Power Generation*. Woodhead Publishing Limited.

Iyogun, K., Lateef, S.A. and Ana, G.R., 2018. Lung Function of Grain Millers Exposed to Grain Dust and Diesel Exhaust in Two Food Markets in Ibadan Metropolis, Nigeria. *Safety and Health at Work*.

Jamrozik, A., Tutak, W. and Ko, M., 2018. Study on co-combustion of diesel fuel with oxygenated alcohols in a compression ignition dual-fuel engine. *Fuel*, 221, pp.329–345.

Lam, S.H. and Goussis, D.A., 1989. Understanding complex chemical kinetics with computational singular perturbation. *Symposium (International) on Combustion*, 22(1), pp.931–941.

Le, M.K. and Kook, S., 2015. Injection pressure effects on the flame development in a light-duty optical diesel engine. *SAE International Journal of Engines*, *8*(2), pp.609-624.

Li, R., Li, S., Wang, F. and Li, X., 2016. Sensitivity analysis based on intersection approach for mechanism reduction of cyclohexane. *Combustion and Flame*, 166, pp.55–65.

Liao, S., Li, H., Mi, L., Shi, X., Wang, G., Cheng, Q. and Yuan, C., 2011. Development and Validation of a Reduced Chemical Kinetic Model for Methanol Oxidation. *Fuel*, 24(1), pp.60–71.

Liu, X., Wang, H., Wang, X., Zheng, Z. and Yao, M., 2017. Experimental and modelling investigations of the diesel surrogate fuels in direct injection compression ignition combustion. *Applied Energy*, 189, pp.187–200.

Lu, T. and Law, C.K., 2005. A directed relation graph method for mechanism reduction. *Proceedings of the Combustion Institute*, 30(1), pp.1333–1341.

Lu, T. and Law, C.K., 2009. Toward accommodating realistic fuel chemistry in large-scale computations. *Progress in Energy and Combustion Science*, 35(2), pp.192–215.

Lu, T.F. and Law, C.K., 2008. Strategies for mechanism reduction for large hydrocarbons: n-heptane. *Combustion and Flame*, 154(1–2), pp.153–163.

Luo, Z., Plomer, M., Lu, T., Som, S., Longman, D.E., Sarathy, S.M. and Pitz, W.J., 2012. A reduced mechanism for biodiesel surrogates for compression ignition engine applications. *Fuel*, *99*, pp.143-153.

Maas, U. and Pope, S.B., 1992. Simplifying chemical kinetics: intrinsic low-dimensional manifolds in composition space. *Combustion and flame*, 88(3-4), pp.239-264.

Metcalfe, W.K., Burke, S.M., Ahmed, S.S. and Curran, H.J., 2013. A Hierarchical and Comparative Kinetic Modeling Study of $C_1 - C_2$ Hydrocarbon and Oxygenated Fuels. *International Journal of Chemical Kinetics*, 45(10), pp.638–675.

Mittal, G. and Sung, C.-J., 2009. Autoignition of methylcyclohexane at elevated pressures. *Combustion and Flame*, 156(9), pp.1852–1855.

Montgomery, C.J., Yang, C., Parkinson, A.R. and Chen, J.Y., 2006. Selecting the optimum quasi-steady-state species for reduced chemical kinetic mechanisms using a genetic algorithm. *Combustion and Flame*, 144(1-2), pp.37-52.

Nakamura, H., Darcy, D., Mehl, M., Tobin, C.J., Metcalfe, W.K., Pitz, W.J., Westbrook, C.K. and Curran, H.J., 2014. An experimental and modeling study of shock tube and rapid compression machine ignition of n-butylbenzene/air mixtures. *Combustion and Flame*, 161(1), pp.49–64.

Narayanaswamy, K., Pepiot, P. and Pitsch, H., 2014. A chemical mechanism for low to high temperature oxidation of n-dodecane as a component of transportation fuel surrogates. *Combustion and Flame*, *161*(4), pp.866-884.

Niemeyer, K.E., Sung, C.J. and Raju, M.P., 2010. Skeletal mechanism generation for surrogate fuels using directed relation graph with error propagation and sensitivity analysis. *Combustion and Flame*, 157(9), pp.1760–1770.

Oehlschlaeger, M.A., Steinberg, J., Westbrook, C.K. and Pitz, W.J., 2009. The autoignition of iso-cetane at high to moderate temperatures and elevated pressures: Shock tube experiments and kinetic modeling. *Combustion and flame*, *156*(11), pp.2165-2172.

Orme, J.P., Curran, H.J. and Simmie, J.M., 2006. Experimental and modeling study of methyl cyclohexane pyrolysis and oxidation. *The Journal of Physical Chemistry A*, 110(1), pp.114-131.

Pepiot-Desjardins, P. and Pitsch, H., 2008. An efficient error-propagation-based reduction method for large chemical kinetic mechanisms. *Combustion and Flame*, 154(1–2), pp.67–81.

Perini, F., Brakora, J.L., Reitz, R.D. and Cantore, G., 2012. Development of reduced and optimized reaction mechanisms based on genetic algorithms and element flux analysis. *Combustion and Flame*, 159(1), pp.103–119.

Petersen, E.L., Kalitan, D.M., Simmons, S., Bourque, G., Curran, H.J. and Simmie, J.M., 2007. Methane/propane oxidation at high pressures: Experimental and detailed chemical kinetic modeling. *Proceedings of the combustion institute*, *31*(1), pp.447-454.

Pitz, W.J., Naik, C. V., Ní Mhaoldúin, T., Westbrook, C.K., Curran, H.J., Orme, J.P. and Simmie, J.M., 2007. Modeling and experimental investigation of methylcyclohexane ignition in a rapid compression machine. *Proceedings of the Combustion Institute*, 31(1), pp.267–275.

Poon, H.M., Ng, H.K., Gan, S., Pang, K.M. and Schramm, J., 2013. Evaluation and development of chemical kinetic mechanism reduction scheme for biodiesel and diesel fuel surrogates. *SAE International Journal of Fuels and Lubricants*, 6(3), pp.729-744.

Poon, H.M., Ng, H.K., Gan, S., Pang, K.M. and Schramm, J., 2014. Development and validation of chemical kinetic mechanism reduction scheme for large-scale mechanisms. SAE International Journal of Fuels and Lubricants, 7(3), pp.653-662.

Poon, H.M., Pang, K.M., Ng, H.K., Gan, S. and Schramm, J., 2016a. Development of multi-component diesel surrogate fuel models - Part I: Validation of reduced mechanisms of diesel fuel constituents in 0-D kinetic simulations. *Fuel*, 180, pp.433–441.

Poon, H.M., Pang, K.M., Ng, H.K., Gan, S. and Schramm, J., 2016b. Development of multi-component diesel surrogate fuel models - Part II: Validation of the integrated mechanisms in 0-D kinetic and 2-D CFD spray combustion simulations. *Fuel*, 181, pp.120–130.

Qian, Y., Yu, L., Li, Z., Zhang, Y., Xu, L., Zhou, Q., Han, D. and Lu, X., 2018. A new methodology for diesel surrogate fuel formulation: Bridging fuel fundamental properties and real engine combustion characteristics. *Energy*, 148, pp.424–447.

Ra, Y. and Reitz, R.D., 2008. A reduced chemical kinetic model for IC engine combustion simulations with primary reference fuels. *Combustion and Flame*, 155(4), pp.713–738.

Rabitz, H., Kramer, M. and Dacol, D., 1983. Sensitivity analysis in chemical kinetics. *Annual review of physical chemistry*, 34(1), pp.419-461.

Rai, P.K. and Rai, P.K., 2016. Adverse Health Impacts of Particulate Matter. *Biomagnetic Monitoring of Particulate Matter*, pp.15–39.

Sankaran, R., Hawkes, E.R., Chen, J.H., Lu, T. and Law, C.K., 2007. Structure of a spatially developing turbulent lean methane–air Bunsen flame. *Proceedings of the combustion institute,* 31(1), pp.1291-1298.

Sarathy, S.M., Westbrook, C.K., Mehl, M., Pitz, W.J., Togbe, C., Dagaut, P., Wang, H., Oehlschlaeger, M.A., Niemann, U., Seshadri, K., Veloo, P.S., Ji, C., Egolfopoulos, F.N. and Lu, T., 2011. Comprehensive chemical kinetic modeling of the oxidation of 2-methylalkanes from C7 to C20. *Combustion and Flame*, 158(12), pp.2338–2357.

Silke, E.J., Pitz, W.J., Westbrook, C.K. and Ribaucour, M., 2007. Detailed chemical kinetic modeling of cyclohexane oxidation. *Journal of Physical Chemistry A*, 111(19), pp.3761–3775.

Sirjean, B., Buda, F., Hakka, H., Glaude, P.A., Fournet, R., Warth, V., Battin-Leclerc, F. and Ruiz-Lopez, M., 2007. The autoignition of cyclopentane and cyclohexane in a shock tube. *Proceedings of the Combustion Institute*, 31(1), pp.277–284.

Sivaramakrishnan, R. and Michael, J. V., 2009. Shock tube measurements of high temperature rate constants for OH with cycloalkanes and methylcycloalkanes. *Combustion and Flame*, 156(5), pp.1126–1134.

Stagni, A., Frassoldati, A., Cuoci, A., Faravelli, T. and Ranzi, E., 2016. Skeletal mechanism reduction through species-targeted sensitivity analysis. *Combustion and Flame*, 163, pp.382–393.

Slavinskaya, N., Saibov, E., Riedel, U., Herzler, J., Naumann, C., Thomas, L. and Saffaripour, M., 2014. Kinetic surrogate model for GTL kerosene. In *52nd Aerospace Sciences Meeting* (p. 0126).

Sung, C.J., Law, C.K. and Chen, J.Y., 2001. Augmented reduced mechanisms for NO emission in methane oxidation. *Combustion and Flame*, *125*(1-2), pp.906-919.

Szymkowicz, P.G. and Benajes, J., 2018. Development of a Diesel Surrogate Fuel Library. *Fuel*, 222, pp.21-34.

Tosatto, L., Bennett, B.A. V. and Smooke, M.D., 2013. Comparison of different DRG-based methods for the skeletal reduction of JP-8 surrogate mechanisms. *Combustion and Flame*, 160(9), pp.1572–1582.

Vajda, S., Valko, P. and Turanyi, T., 1985. Principal component analysis of kinetic models. *International Journal of Chemical Kinetics*, 17(1), pp.55-81.

Valorani, M., Creta, F., Goussis, D.A., Lee, J.C. and Najm, H.N., 2006. An automatic procedure for the simplification of chemical kinetic mechanisms based on CSP. *Combustion and Flame*, *146*(1-2), pp.29-51.

Vanderover, J. and Oehlschlaeger, M.A., 2009. Ignition time measurements for methylcylcohexane- and ethylcyclohexane-air mixtures at elevated pressures. *International Journal of Chemical Kinetics*, 41(2), pp.82–91.

Vasu, S.S., Davidson, D.F., Hong, Z. and Hanson, R.K., 2009. Shock Tube Study of Methylcyclohexane Ignition over a Wide Range of Pressure and Temperature. *Energy & Fuels*, 23(1), pp.175–185.

Wang, Z., 2018. Experimental and Kinetic Modeling Study of Cyclohexane and Its Mono-alkylated Derivatives Combustion. Springer.

Wang, H. and Frenklach, M., 1991. Detailed reduction of reaction mechanisms for flame modeling. *Combustion and Flame*, 87(3-4), pp.365-370.

Weber, B.W., Pitz, W.J., Mehl, M., Silke, E.J., Davis, A.C. and Sung, C.J., 2014. Experiments and modeling of the autoignition of methylcyclohexane at high pressure. *Combustion and Flame*, 161(8), pp.1972–1983.

Westbrook, C.K., Pitz, W.J., Herbinet, O., Curran, H.J. and Silke, E.J., 2009. A comprehensive detailed chemical kinetic reaction mechanism for combustion of n-alkane hydrocarbons from n-octane to n-hexadecane. *Combustion and flame*, *156*(1), pp.181-199.

Xin, Y., Sheen, D.A., Wang, H. and Law, C.K., 2014. Skeletal reaction model generation, uncertainty quantification and minimization: Combustion of butane. *Combustion and Flame*, 161(12), pp.3031–3039.

Yang, J., Johansson, M., Naik, C., Puduppakkam, K., Golovitchev, V. and Meeks, E., 2012. *3D CFD modeling of a biodiesel-fueled diesel engine based on a detailed chemical mechanism* (No. 2012-01-0151). SAE Technical Paper.

Yang, Y. and Boehman, A.L., 2009. Experimental study of cyclohexane and methylcyclohexane oxidation at low to intermediate temperature in a motored engine. *Proceedings of the Combustion Institute*, 32(1), pp.419-426.

Zhang, H.R., Huynh, L.K., Kungwan, N., Yang, Z. and Zhang, S., 2007. Combustion modeling and kinetic rate calculations for a stoichiometric cyclohexane flame. 1. Major reaction pathways. *The Journal of Physical Chemistry A,* 111(19), pp.4102-4115.

Zheng, X.L., Lu, T.F. and Law, C.K., 2007. Experimental counterflow ignition temperatures and reaction mechanisms of 1, 3-butadiene. *Proceedings of the Combustion Institute*, 3(1), pp.367-375.

APPENDICES

APPENDIX A: Species Considered in the Reduced Models

```
--------------------------------------------------------------------------------
                     SPECIES CONSIDERED IN MCHv1
--------------------------------------------------------------------------------
    1    H        31   CH3CHO      61   C5H5
    2    H2       32   CH3CO       62   C5H4O
    3    O        33   CH2CHO      63   C5H3O
    4    O2       34   CH2CO       64   C6H5CH2
    5    OH       35   HCCO        65   C6H5CH3
    6    H2O      36   CH3CO3H     66   C6H4CH3
    7    N2       37   CH3CO3      67   CYCHEXENE
    8    HO2      38   C2H5O       68   MCHR2
    9    H2O2     39   C2H5O2H     69   MCHR3
   10    CO       40   C2H5O2      70   MCH
   11    CO2      41   C2H4O1-2    71   KC7H13G
   12    CH2O     42   C2H3CHO     72   MCH2OO
   13    HCO      43   C2H3CO      73   MCH3OO
   14    HCOH     44   C3H6        74   MCH2QX
   15    HOCHO    45   C3H5-A      75   MCH3QJ1
   16    OCHO     46   C3H4-A      76   C7ENE-ONE
   17    CH3OH    47   C3H3        77   C7ENE-ONEJ
   18    CH2OH    48   C3H5O       78   MCH2QXQJ
   19    CH3O     49   H2CC        79   MCH2OXQ
   20    CH3O2H   50   C4H6        80   MCH2OXOJ
   21    CH3O2    51   C4H4        81   CHXRAD
   22    CH4      52   C4H2        82   CHX1*O2J
   23    CH3      53   C4H5-N      83   C6H11-16
   24    CH2      54   C5H91-4     84   CYHX1N3J
   25    CH2(S)   55   C6H11       85   CYHX13ENE
   26    C2H5     56   C6H6        86   CYHX13N5J
   27    C2H4     57   C5H6
   28    C2H3     58   C6H5
   29    C2H2     59   C6H5O
   30    C2H      60   C6H5OH
--------------------------------------------------------------------------------
```

Figure A-1: Species Considered in MCHv1 Mechanism

```
--------------------------------------------------------------------------------
                     SPECIES CONSIDERED IN MCHv2
--------------------------------------------------------------------------------
    1    H        31   CH3CO       61   C5H5O
    2    H2       32   CH2CHO      62   C5H5OH
    3    O        33   CH2CO       63   C5H4OH
    4    O2       34   HCCO        64   C5H3O
    5    OH       35   CH3CO3H     65   C6H5OO
    6    H2O      36   CH3CO3      66   C5H7
    7    N2       37   C2H5OH      67   MCHR2
    8    HO2      38   C2H5O       68   MCH
    9    H2O2     39   C2H5O2H     69   MCH2OO
   10    CO       40   C2H5O2      70   MCH2QX
   11    CO2      41   C2H4O2H     71   MCH2QXQJ
   12    CH2O     42   C2H3CHO     72   MCH2OXQ
   13    HCO      43   C2H3CO      73   MCH2OXOJ
   14    HOCHO    44   C2H5CHO     74   CHXRAD
   15    OCHO     45   C2H5CO      75   CHX1*O
   16    CH3OH    46   C3H6        76   CHX1*O2J
   17    CH2OH    47   C3H3        77   C6H11-16
   18    CH3O     48   C3H5O
   19    CH3O2H   49   C4H6
   20    CH3O2    50   C4H4
   21    CH4      51   C4H2
   22    CH3      52   C4H4O
   23    CH2      53   C6H11
   24    C2H5     54   C6H6
   25    C2H4     55   C5H6
   26    C2H3     56   C6H5
   27    C2H2     57   C6H5O
   28    C2H      58   C6H5OH
   29    CH3CHO   59   C5H5
   30    C2H3OH   60   C5H4O
--------------------------------------------------------------------------------
```

Figure A-2: Species Considered in MCHv2 Mechanism

```
--------------------------------------------------------------------------------
                       SPECIES CONSIDERED IN D_144
--------------------------------------------------------------------------------
    1   H          31  CH3CHO     61  C5H5        91  PC4H9       121 IC4H8
    2   H2         32  CH3CO      62  C5H4O       92  NC4H9CHO    122 AC12H25
    3   O          33  CH2CHO     63  C5H3O       93  NC4H9CO     123 IC4H7
    4   O2         34  CH2CO      64  C6H5CH2     94  C6H12-1     124 HMN-R1O2
    5   OH         35  HCCO       65  C6H5CH3     95  C16H33-5    125 HMN-R8O2
    6   H2O        36  CH3CO3H    66  C6H4CH3     96  C11H23-1    126 HMNOOH1-2
    7   N2         37  CH3CO3     67  CYCHEXENE   97  C10H21-1    127 HMNOOH8-5
    8   HO2        38  C2H5O      68  MCHR2       98  C9H19-1     128 HMNOOH1-2O2
    9   H2O2       39  C2H5O2H    69  MCHR3       99  C8H17-1     129 HMNOOH8-5O2
   10   CO         40  C2H5O2     70  MCH         100 C7H15-1     130 HMNKET1-2
   11   CO2        41  C2H4O1-2   71  KC7H13G     101 C6H13-1     131 HMNKET8-5
   12   CH2O       42  C2H3CHO    72  MCH2OO      102 C5H11-1     132 IC3H6CHO
   13   HCO        43  C2H3CO     73  MCH3OO      103 C16H33O-5   133 AC11H23
   14   HCOH       44  C3H6       74  MCH2QX      104 C16H33O2-5  134 CC8H17
   15   HOCHO      45  C3H5-A     75  MCH3QJ1     105 C9H19O2-1   135 CH3COCH2
   16   OCHO       46  C3H4-A     76  C7ENE-ONE   106 C16OOH5-7   136 TC4H8CHO
   17   CH3OH      47  C3H3       77  C7ENE-ONEJ  107 C9OOH1-3    137 DC8H17
   18   CH2OH      48  C3H5O      78  MCH2QXQJ    108 C16OOH5-7O2 138 CC9H19
   19   CH3O       49  H2CC       79  MCH2OXQ     109 C9OOH1-3O2  139 PC7H15
   20   CH3O2H     50  C4H6       80  MCH2OXOJ    110 C16KET5-7   140 NEOC5H11
   21   CH3O2      51  C4H4       81  CHXRAD      111 C9KET1-3    141 NEOC5H11O
   22   CH4        52  C4H2       82  CHX1*O2J    112 NC9H19CHO   142 C3H5-T
   23   CH3        53  C4H5-N     83  C6H11-16    113 NC6H13CHO   143 IC4H7O
   24   CH2        54  C5H91-4    84  CYHX1N3J    114 NC9H19CO    144 IC4H8O
   25   CH2(S)     55  C6H11      85  CYHX13ENE   115 NC6H13CO
   26   C2H5       56  C6H6       86  CYHX13N5J   116 HMN-R1
   27   C2H4       57  C5H6       87  C16H34      117 HMN-R8
   28   C2H3       58  C6H5       88  C2H6        118 HMN
   29   C2H2       59  C6H5O      89  NC3H7       119 TC4H9
   30   C2H        60  C6H5OH     90  NC4H9COCH2  120 FC12H25
--------------------------------------------------------------------------------
```

Figure A-3: Species Considered in D_144 Mechanism